


# A geochemical approach to distinguishing competing tectono-magmatic processes preserved in small eruptive centres

Lucy E. McGee<sup>1,2,6</sup>  · Raimundo Brahm<sup>1,2</sup> · Michael C. Rowe<sup>3</sup> · Heather K. Handley<sup>4</sup> · Eduardo Morgado<sup>1,2,7</sup> · Luis E. Lara<sup>5</sup> · Michael B. Turner<sup>4</sup> · Nicolas Vinet<sup>1,2</sup> · Miguel-Ángel Parada<sup>1,2</sup> · Pedro Valdivia<sup>2</sup>

Received: 4 October 2016 / Accepted: 13 April 2017 / Published online: 23 May 2017  
© Springer-Verlag Berlin Heidelberg 2017

**Abstract** Small eruptive centres (SECs) representing short-lived, isolated eruptions are effective samples of mantle heterogeneity over a given area, as they are generally of basaltic composition and show evidence of little magmatic processing. This is particularly powerful in volcanic arcs where the original melting process generating stratovolcanoes is often obscured by additions from the down-going slab (fluids and sediments) and the overlying crust. The Pucón area of southern Chile contains active and dormant stratovolcanoes, Holocene, basaltic SECs and an arc-scale strike-slip fault (the Liquiñe Ofqui Fault System: LOFS).

The SECs show unexpected compositional heterogeneity considering their spatial proximity. We present a detailed study of these SECs combining whole rock major and trace element concentrations, U-Th isotopes and olivine-hosted melt inclusion major element and volatile contents to highlight the complex inter-relations in this small but active area. We show that heterogeneity preserved at individual SECs relates to different processes: some start in the melting region with the input of slab-derived fluids, whilst others occur later in a centre's magmatic history with the influence of crustal contamination prior to olivine crystallisation. These signals are deduced through the combination of the different geochemical tools used in this study. We show that there is no correlation between composition and distance from the arc front, whilst the local tectonic regime has an effect on melt composition: SECs aligned along the LOFS have either equilibrium U-Th ratios or small Th-excesses instead of the large—fluid influenced—U-excesses displayed by SECs situated away from this feature. One of the SECs is modelled as being generated from fluid-enriched depleted mantle, a source which it may share with the stratovolcano Villarrica, whilst another SEC with abundant evidence of crustal contamination may share its plumbing system with its neighbouring stratovolcano Quetupillán, showing that polygenetic—monogenetic connections are unpredictable. Such marked preservation of individual magmatic histories highlights the isolation of individual melting events even in complex and highly volcanically active areas.

Communicated by Timothy L. Grove.

**Electronic supplementary material** The online version of this article (doi:[10.1007/s00410-017-1360-2](https://doi.org/10.1007/s00410-017-1360-2)) contains supplementary material, which is available to authorized users.

✉ Lucy E. McGee  
lucy.mcgee@mq.edu.au

- <sup>1</sup> Centro de Excelencia en Geotermia de los Andes (CEGA), Santiago, Chile
- <sup>2</sup> Department of Geology, Universidad de Chile, Plaza Ercilla 803, Santiago, Chile
- <sup>3</sup> School of Environment, University of Auckland, Private Bag 92019, Auckland, New Zealand
- <sup>4</sup> Department of Earth and Planetary Sciences, Macquarie University, Sydney, Australia
- <sup>5</sup> Volcano Hazards Program, Servicio Nacional de Geología y Minería (SERNAGEOMIN), Santiago, Chile
- <sup>6</sup> Present Address: Department of Earth and Planetary Sciences, Macquarie University, Sydney, Australia
- <sup>7</sup> Present Address: Institute of Geophysics and Tectonics, School of Earth and Environment, University of Leeds, Leeds, UK

**Keywords** Southern Chile · U-Th isotopes · Heterogeneity · Monogenetic · Melt inclusions · Tectonics

## Introduction

Studies over the past decade of small volume volcanic events have shown that the erupted products are rarely homogeneous, or chemically ‘monogenetic’, despite falling into this category in terms of physical volcanology (e.g. Brenna et al. 2010; Haase and Renno 2008; McGee and Smith 2016; Rasoazanamparany et al. 2015; Strong and Wolff 2003). Well-preserved, accessible volcanic sequences representing short-lived basaltic eruptions provide a snapshot in time of source compositions, melting and ascent processes over a small spatial footprint, and thus can provide important information regarding basaltic melt generation which cannot be obtained from longer-lived, less accessible stratovolcano sequences. This asset can be utilised to great effect in tectonically complex areas such as continental margins, where the geochemical effects of the various subduction zone inputs may be interwoven with signals imprinted by regional structure.

Unlike intraplate fields of small eruptive centres (SECs) such as those found in New Zealand, Australia and central Europe, the interplay of local and arc-scale tectonic features in subduction settings can have a profound effect on the composition of resultant melt batches in terms of source and slab inputs, time for fractional crystallisation and/or assimilation of crustal lithologies and ascent along compressive/extensional domains (e.g. Cembrano and Lara 2009). While numerous studies have focused on the geochemical attributes of basaltic eruptions of stratovolcanoes in continental subduction zones (e.g. Gamble et al. 1999; Leeman et al. 2005; Price et al. 2010; Reagan and Gill 1989; Ruprecht et al. 2012), relatively few have specifically targeted volcanic fields composed of small volume volcanoes in such settings, e.g. the Chichinautzen volcanic field, Mexico (Siebe et al. 2004; Wallace and Carmichael 1999) and the Cascades range, USA (Borg et al. 1997; Conrey et al. 1997; Rowe et al. 2009). The advantage of focusing on small basaltic eruptions is that their geochemical compositions are more likely to represent the complexity of source and ascent processes and their environment. Additionally, their small size means that high resolution sampling is often possible through all stages of the eruption (e.g. Blondes et al. 2008; Brenna et al. 2012; Jordan et al. 2015; McGee et al. 2012), revealing features which may be missed in stratovolcanoes.

Many fields of Holocene basaltic SECs in Central and Southern Chile are situated in close proximity to active or dormant stratovolcanoes, and the connection between these two eruption types has been the topic of numerous recent studies both from a tectonic (Bucchi et al. 2015; Cembrano and Lara 2009) and petrologic (Hickey-Vargas et al. 2002, 2016; Jacques et al. 2014; Jicha et al. 2007;

Morgado et al. 2015; Wehrmann et al. 2014) perspective. It has been recognised that Chilean stratovolcanoes have different sources and inputs/processes to their neighbouring SECs. Some of this is hypothesised as related to the physical location of the volcanoes and SEC fields (e.g. Hickey-Vargas et al. 2016; Watt et al. 2013; Wehrmann et al. 2014). Our study, however, shows that there are differences even within small fields of SECs that cannot be related to position in the arc front, and that may be caused by competing tectonic and magmatic processes and how or if the chemical signals of these are preserved.

We present a large, high resolution dataset of eruption sequences from five Holocene basaltic SECs in the Pucón area of Southern Chile, which lie in close proximity to the active stratovolcano Villarrica. Whole rock major and trace element and U-Th isotopic analyses combined with olivine-hosted melt inclusion compositions reveal a complex interplay between fluid-flux melting, overprinting with decompression melting signals and crustal contamination affecting individual centres. We show that although some geochemical signatures can be attributed to tectonics, there is no correlation between subduction component input, partial melting degree and distance from the arc front, suggesting that small volume melt batches are isolated along-arc and affected uniquely by melting and ascent-related processes (such as mixing of melts, fractional crystallisation and crustal contamination). Similar geochemical ‘flavours’ are found in other areas of Southern Chile, suggesting that the heterogeneity observed in this one small region is present on a larger scale, but the small size of the melt batches led to these being preserved in the individual SECs. Further support for this is in compositional similarities with Villarrica literature analyses which show that magmas forming the stratovolcano may have been affected by some of the same processes as the individual SECs but these are diluted or homogenised with time, increased magma volumes, and the effects of magma evolution.

## Setting and background

The Pucón area of Southern Chile is within the Central part of the Southern Volcanic Zone (SVZ) of the Andes (33–46°S), a volcanic chain caused by subduction of the Nazca plate since 30 Ma beneath the South American plate. This area is well-populated with both stratovolcanoes and SECs which have been active throughout the Holocene. Several of these stratovolcanoes have been the subject of detailed geochemical studies and are used in the present study as a comparison to the Pucón area due to their close proximity, similar rock compositions (basalt to andesite), a similar underlying crustal thickness (30–40 km) and the same basement rock types. A brief summary is provided

here and their locations are shown on Fig. 1a. Volcán Llaïma (38.7°S) is one of the most historically active volcanoes in South America and ended its most recent eruptive phase in 2009. Rocks produced are of basalt to andesite composition, and despite having little geochemical evidence of crustal contamination in Sr–Nd–Pb–O isotopic ratios, U-series isotopic modelling by Reubi et al. (2011) revealed assimilation of the plutonic roots of the complex. Crustal contamination by basement (silicic intrusive) rock types was modelled as a dominant process at Volcán Mocho-Choshuenco (40°S); as with Volcán Llaïma this was revealed not through Sr–Nd–Pb–O isotopic ratios but trace element ratio modelling, and corroborated by the presence of partially melted granitic xenoliths within lavas (McMillan et al. 1989). Volcán Lonquimay (38.2°S) lacks a detailed study, although has been included in several recent geochemical studies of the central SVZ who observed that rock compositions extend to trachyandesites (Jacques et al. 2014), and that magmas may be produced from a depleted source similar to that of Villarrica, seen through low Cl contents in olivine-hosted melt inclusions (Wehrmann et al. 2014). Such studies show the value of combining geochemical techniques in order to elucidate complex magmatic processes. The stratovolcanoes Villarrica, Quetrupillán and Lanín lie on a northwest-southeast lineation with approximately 20 km between each. Quetrupillán and Lanín have erupted rocks with compositions ranging from andesite to dacite and basalt to high silica andesite, respectively, whilst

Villarrica rock compositions are more mafic, ranging from basalt to andesite (Hickey-Vargas et al. 1989).

The area 15–20 km to the north and northeast of Villarrica volcano contains eight volcanic complexes of basaltic SECs: Caburgua, La Barda, Huelemolle, Redondo, Cañi, Relicura, San Jorge and Huililco (Fig. 1). Caburgua, La Barda and Huelemolle are all situated in-line with the approximately north–south orientated Liquiñe-Ofqui fault system (LOFS) (Cembrano et al. 1996), an intra-arc, transpressional strike-slip fault that runs for approximately 1200 km in southern Chile; several SECs are aligned with this feature (Cembrano et al. 1996; Cembrano and Lara 2009; Lara et al. 2006; López-Escobar et al. 1995). The SECs Relicura, Cañi and Redondo lie along a north-northeast–south-southwest lineament, whilst San Jorge and Huililco are not related to any regional or local structural feature. Caburgua and La Barda volcanic centres lie opposite each other, separated by the LOFS-orientated Lake Caburgua (Fig. 1).

The volcanic complexes take the form of small scoria cones with associated lava flows, ranging in volume from 0.004 km<sup>3</sup> (San Jorge) to 4.69 km<sup>3</sup> (La Barda)—see Morgado et al. (2015) for a full list of calculated dimensions of the SECs. Huelemolle, Caburgua and La Barda each consist of three small, overlapping cones which are aligned along possible short fissures (Fig. 1b). This alignment and the shapes of the cones suggest that all vents for each of these centres were active contemporaneously or erupted within a geological short space of time. San Jorge and Huililco,

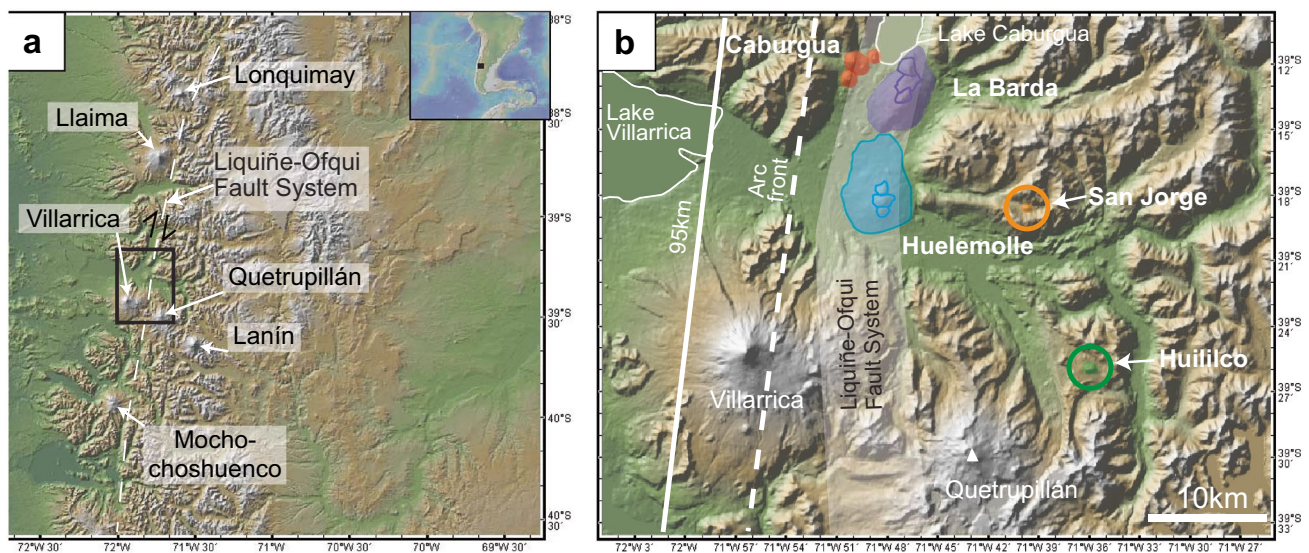


**Fig. 1** **a** Large-scale location map of the Central Southern Volcanic Zone of Chile showing the location of stratovolcanoes mentioned in this study. The study area is marked by the *black box*. **b** The location of the small eruptive centres (SECs) investigated in this study. The stratovolcanoes Quetrupillán and Villarrica and the Liquiñe Ofqui

fault system (LOFS) are also shown. The *white dashed line* shows the arc front at 100 km slab depth, the *solid white line* shows 95 km slab depth (from Tašárová 2007). Maps were modified from the GeoMap app

however, are each composed of a single scoria cone and lava flows (one single flow to the west in the case of San Jorge, and two north and south flows in the case of Huililco). The majority of the SECs overlie Cretaceous to Miocene granitoids, although Paleocene volcanoclastic sediments and lavas crop-out in the east of the area, and may lie beneath Relicura. San Jorge appears to be situated on the contact between this unit and Cretaceous granitoids. Huililco is underlain by Miocene granitoids and possibly Pliocene volcanoclastic rocks which outcrop ca. 5 km south of the volcanic centre (Cembrano and Lara 2009). Villarrica has been active since the Pleistocene, and most recently erupted in 2015, 1984 and 1971. All SECs are Holocene in age as they show no effects of glacial erosion. Caburgua, La Barda, Huelemolle and Redondo are thought have erupted sometime between the two main ignimbrite pulses of Villarrica at 4 and 14 ka (Hickey-Vargas et al. 2002), but ages are not constrained from the other SECs. The fresh, unweathered nature of the San Jorge fall deposits—along with its U-Th isotopic characteristics (see later)—suggests that this centre is relatively young (<6 ka).

## Analytical methods

Table 1 summarises the data reported in this study. 67 new, whole rock major and trace element analyses were obtained on lapilli, scoria, bomb and lava samples collected in July

2014, January 2015 and October 2015. These data are supplemented in our figures and discussion with 19 analyses of lava samples from three of the SECs and the 1971 eruption of the stratovolcano Villarrica previously reported in Morgado et al. (2015), 16 analyses of lava samples from inter- and postglacial and historic eruptions of Villarrica previously reported in Hickey-Vargas et al. (1989), and four Holocene to recent tephra samples from Wehrmann et al. (2014). We use previously reported whole rock Sr–Nd isotopic data for the SECs and Villarrica from Morgado et al. (2015) and Hickey-Vargas et al. (1989, 2002, 2016). We report the results of 19 new whole rock U-Th isotopic analyses for the SECs and the 2015 eruption of Villarrica. We do not use the U-Th analyses for Villarrica and nearby SECs reported in Hickey-Vargas et al. (2002) as these were analysed by a different method (alpha spectroscopy) and the ratios of individual centres cannot be resolved within the associated error bars. Melt inclusion analyses and associated olivine major element data were obtained on three samples from three SECs (Caburgua, San Jorge and Huililco) specifically for this study.

Whole rock major and trace element analyses for this study were undertaken at the commercial laboratory Actlabs Inc. (Canada) over three sessions (September 2014, April 2015 and October 2015). Major elements and the trace elements Sc, V, Ba, Sr, Y, Zr were analysed by fusion inductively coupled plasma (ICP) analysis. Samples were mixed with a flux of lithium metaborate and lithium

**Table 1** Summary of the data and sources used in this study

Volcano	Whole rock data			Melt inclusions
	Majors and traces	Sr–Nd isotopes	U–Th isotopes	
Huelemolle	5 lava, 3 from <sup>a</sup>	1 <sup>a</sup> 1 <sup>b</sup>	3 lava	
Caburgua	15 scoria and bombs <sup>a</sup> 5 lava	1 <sup>a</sup> 4 <sup>b</sup>	3 lava	1 scoria (LEM-CB-9)
La Barda	8 scoria 9 lava (4 from <sup>a</sup> )	1 <sup>a</sup> 2 <sup>b</sup>	1 scoria 2 lava	
Huililco	5 scoria/lapilli 2 bombs 11 lava	2 <sup>b</sup>	1 bomb 2 lava	1 lapilli (PVM-15B)
San Jorge	12 scoria/lapilli 3 bombs 6 lava	1 <sup>a</sup> 3 <sup>b</sup>	2 scoria 1 bomb 3 lava	1 lapilli (SJ-T-3a)
Villarrica	<sup>a</sup> 5 lava (1971) <sup>b</sup> 16 lava (interglacial to 1984) <sup>c</sup> 4 Holocene to recent tephra 1 spatter (2015)	5 <sup>b</sup>	<sup>d</sup> 2 lava 1 (2015)	

Italics denotes this study

<sup>a</sup> Morgado et al. (2015)

<sup>b</sup> Hickey-Vargas et al. (1989, 2002 or 2016)

<sup>c</sup> Wehrmann et al. (2014)

<sup>d</sup> Sigmarsson et al. (2002) (plotted in Fig. 5)

tetraborate and fused in a furnace; the liquid sample was then mixed into a 5% HNO<sub>3</sub> solution containing an internal standard, and analysed on a Thermo Jarrell-Ash ENVIRO II ICP mass spectrometer (MS). These solutions were then diluted and analysed for trace element content (Cr, Co, Ni, Cu, Zn, Ga, Rb, Nb, Cs, La, Ce, Pr, Nd, Sm, Eu, Gd, Tb, Dy, Ho, Er, Tm, Yb, Lu, Hf, Ta, Pb, Th, U) on a Perkin Elmer Sciex ELAN ICP MS. A method blank using the same reagents as for samples was analysed in every session, and values obtained for all elements are below detection limit. The reference materials BCR-2 and BHVO-2 were analysed and measured as unknowns within each session; these data are reported in the electronic appendix. Accuracy for major elements in both standards is better than 3% except for MgO in BHVO-2 which is 4.4%. Ta concentrations in the samples are very close to the detection limit and show a large amount of scatter, therefore this element is not plotted in any figure. Accuracy in the trace elements in BHVO-2 ( $n = 2$ ) and BCR-2 ( $n = 3$ ) is better than 10% except in Y (17 and 19%, respectively), Ni (12 and 63%, respectively), Ga (13% for both) and Nb (14 and 18%, respectively). In BHVO-2 Cr has an error of 20% and Gd an error of 13%, and in BCR-2 Cu has an error of 37%, Hf an error of 11% and Pb an error of 12%. The Pb reference value in BHVO-2 is below the limit of detection for Actlabs (5 ppm); therefore, the quality of the Pb analysis in this standard cannot be reported. Based on these statistics, we report but do not plot or interpret concentrations of Y, Ni, Cu, Ga or Pb. For all other elements with accuracy of >10% error, we take into account the maximum error bar in their interpretation. Three duplicates were prepared and analysed in session 1 and 1 in session 2, and are generally in excellent agreement with originals, with the exception of Pb in every session (values very close to detection limit), a difference of 20% in Cr, 11% in Nb, 15% in Hf, 33% in Y, of 12.5% in Zn and Rb and 14% in U in the first session. A difference of 40% in TiO<sub>2</sub> and 70% in Th is reported in one duplicate from session 1, but as the other two duplicates show excellent agreement (1.3 and 0.1%, and 0%, respectively) we suggest that this error is not present in the whole dataset for this session.

U and Th isotopic ratios were determined on bulk rock powders using the procedure employed by the U-series Research Laboratory at Macquarie University for volcanic rock samples. Samples were chosen to represent the most mafic samples of all phases of each eruption, where possible (Table 1). Approximately, 0.3 g of powdered rock was spiked with a <sup>236</sup>U-<sup>229</sup>Th tracer and digested in a mixture of concentrated acids (HF-HNO<sub>3</sub>). Separation of U and Th followed standard anionic resin chromatography as described in Turner et al. (2011). Uranium and thorium concentrations, determined by isotope dilution, and U-Th isotope ratios were measured

separately on a Nu Instrument Multi-Collector ICP-MS at Macquarie University following the approach detailed by Turner et al. (2011). The New Brunswick Laboratory (NBL) synthetic standards U010 and U005a were used at regular intervals to assess the robustness of instrumental corrections and to monitor drift. A standard-sample bracketing procedure for each sample analysed used the Th 'U' standard solution, and a linear tail correction for the <sup>232</sup>Th tail on <sup>230</sup>Th was applied. The rock standard BCR-2 was measured as (<sup>230</sup>Th/<sup>232</sup>Th) = 0.881 ± 0.002, and (<sup>238</sup>U/<sup>232</sup>Th) = 0.885 ± 0.002 (the average of three separate digestions—see electronic appendix) which are within error of values published in Turner et al. (2011) [(<sup>230</sup>Th/<sup>232</sup>Th) = 0.877 ± 0.005, (<sup>238</sup>U/<sup>232</sup>Th) = 0.884 ± 0.018]. A duplicate run of the same solution of one of the samples gave an identical (<sup>230</sup>Th/<sup>232</sup>Th) ratio, and (<sup>238</sup>U/<sup>232</sup>Th) within 2% [HUEL-6: (<sup>230</sup>Th/<sup>232</sup>Th) = 0.962, (<sup>238</sup>U/<sup>232</sup>Th) = 0.952 and 0.949].

Olivine-hosted melt inclusion analyses are generally undertaken on fine-grained, primitive tephra samples to avoid the effects of post entrapment crystallisation (PEC) and re-equilibration (e.g. Rowe et al. 2009). For this reason, the most primitive sample of tephra from three SECs where there was a known tephra phase were chosen for analysis (San Jorge lapilli, Huililco lapilli and Caburgua fine scoria). Olivines were separated at the Universidad de Chile. Tephra samples were washed, dried and rough-crushed before passing through a magnetic separator and heavy liquids, and washed with acetone then distilled water. Melt inclusions in separated olivines varied from containing glassy to partially crystallised inclusions. Melt inclusions were re-homogenised at 1 atm in a Deltech vertical furnace following the procedure described by Rowe et al. (2006). Inclusions were held at near-liquidus temperatures, calculated from bulk rock compositions using COMAGMAT (Ariskin et al. 2012), for c. 10 min to ensure re-homogenisation, and then rapidly quenched. Olivines were bulk-mounted in epoxy and polished to expose the inclusions. Approximately 10 inclusions which were completely re-homogenised were chosen for analysis in each sample. Major elements and volatiles (S and Cl) were analysed on a Cameca SX-100 electron microprobe at Oregon State University. A 7 µm beam was used for the inclusions, and a focused (~1 µm) beam for the host olivine grain. Beam conditions were 15 keV accelerating voltage and 30 nA (for glass) and 50 nA (for mineral phases). A zero-time intercept correction was applied for Na, K, and Si concentrations. The analytical procedure for glass was optimized for analysis of S (120 s peak count time) and Cl (120 s peak count time). Replicate analyses of VG-A99 basalt glass standard were run to monitor instrument calibration and VG-2 basalt glass standard was run as a secondary standard for accuracy and reproducibility over the

duration of the analytical session. Duplicate analyses were conducted on a single large melt inclusion, demonstrating inclusion homogeneity and analytical reproducibility. Because of the basic assumption of olivine-melt equilibrium, one of the challenges associated with olivine-hosted melt inclusions is identifying and correcting for post-entrapment re-equilibration (Fe-loss) and crystallisation (Danyushevsky et al. 2000). This is particularly true for rehomogenised melt inclusions in which temperatures of rehomogenisation may be slightly over/under-estimated. Rowe et al. (2011a) demonstrate a graphical technique for assessing these two competing processes in which measured melt inclusion  $\text{FeO}^*$  and  $\text{MgO}$  concentrations are compared to olivine-melt  $\text{KD}^{\text{Fe}-\text{Mg}}$ . This approach is used here to evaluate the relative effects of melt inclusion-host re-equilibration and over/under heating and demonstrate that inclusions which are outside the range of  $0.3 \pm 0.03$  for olivine-melt  $\text{KD}^{\text{Fe}-\text{Mg}}$  (Roeder and Emslie 1970) are a result of slight overheating. Melt inclusion compositions were thus recalculated based upon the assumed equilibrium composition relative to their host olivine, by incrementally adding or removing olivine to the melt composition until an olivine-melt  $\text{KD}^{\text{Fe}-\text{Mg}}$  of 0.3 was reached (Roeder and Emslie 1970; Sobolev and Chaussidon 1996), see online appendix. 10% ferric iron was assumed for corrections. Calculations were remade at 15% to test the potential effect of oxidation and do not affect minor element abundances and ratios used in this work outside the error of analysis. For the Huililco and Cabargua samples (PVM-15b and CB-9, respectively) little correction was needed (less than 5% in almost all cases), showing that the initial equilibrium conditions were well estimated, whilst the San Jorge sample (SJ-T-3a) required larger corrections (−12 to 6.4% olivine adjustment by wt%). Only one analysis from naturally quenched melt inclusions from sample PVM-15b records significant degassing. In contrast, 50% of the rehomogenised inclusions originally analysed were degassed. Note that only intact melt inclusions (undegassed) are reported in this study to avoid potential chemical exchange between the melt and melt inclusion (Nielsen et al. 1998).

## Samples and petrography

Previous studies of basaltic SECs have identified that geochemical heterogeneity is observed when all phases of the eruption are sampled and analysed (McGee et al. 2012; Rasoazanamparany et al. 2015; Strong and Wolff 2003), therefore all possible types of material were collected where present, in situ and where provenance could be accurately determined. For San Jorge, lapilli were collected through an exposed sequence, and lava samples were collected along the single lava flow. For Huililco,

lapilli, bombs and lava from two short flows were collected. Lava samples already existed for Cabargua and La Barda (Morgado et al. 2015); therefore, scoria and bombs only were collected from all three cones of the Cabargua eruptive centre, and scoria, spatter and some additional lava samples were collected from two of the cones of La Barda. No tephra phase is preserved for Huelemolle; however, two previously unanalysed lava samples collected by E. Morgado were added to augment the pre-existing data. A sample of spatter from the 2015 eruption of Villarrica was donated for this study.

All studied lavas contain olivine, clinopyroxene and plagioclase as phenocrysts and micro-phenocrysts, in a finely crystalline groundmass. Lapilli, scoria and bombs contain olivine as the major phenocryst phase, with plagioclase and clinopyroxene occurring as micro-phenocrysts or groundmass phases. Cr-spinels are present as micro-phenocrysts and within olivine crystals, and have particularly high Cr values (up to 45 wt%) in San Jorge samples (McGee et al. *in prep*). Cr-spinels as inclusions in olivines were observed in 1971 Villarrica lavas, although groundmass and microphenocrysts oxides are titanomagnetite (Morgado et al. 2015). Thus far, no hydrous mineral phases such as amphibole have been identified in eruptive phases from the SECs or Villarrica. Basalts and basaltic andesites from Villarrica contain the same phenocryst phases as the SECs but with modally more plagioclase (Hickey-Vargas et al. 1989). The 2015 spatter sample is vesicle-rich and aphyric. An in-depth study of the petrography and textures of lavas erupted from Cabargua, Huelemolle and San Jorge in comparison to the 1971 lava flow of Villarrica was made by Morgado et al. (2015) in order to calculate pre- and syn-eruptive temperatures and pressures of these systems. The authors suggested the presence of a reservoir at the base of the lower crust for the SECs in comparison with Villarrica which requires at least two stages of crystallisation in deep and shallow reservoirs, showing a profound difference in the plumbing systems of these neighbouring complexes. The petrology of Villarrica units has also been described by Costantini et al. (2011), Pioli et al. (2015) and Witter et al. (2004). A ubiquitous feature of the SECs is that the lava samples in all studied centres contain glomerocrysts of the above mineral phases, sometimes measuring up to several millimetres. The crystals within these have the same composition as the phenocryst phases, with the exception of Huililco (Morgado, Brahm, Vinet and McGee unpublished data). Huililco is anomalous petrographically in the SECs in this area, as it is the only centre in which crystals within lava samples display disequilibrium features: plagioclase phenocrysts commonly have clean or sieve-textured cores and normally and reverse-zoned rims (Valdivia Muñoz, unpublished honors thesis).

## Geochemistry

### Whole rock major and trace elements

Representative data are shown in Table 2 and were selected to show the range of compositions for each eruptive centre as well as type of erupted material. All data are presented in the electronic appendix. All studied rocks are alkali basalts to basaltic andesites with SiO<sub>2</sub> contents ranging from 48.9 to 54 wt%. The SECs excluding San Jorge have a restricted range in total alkalis (Na<sub>2</sub>O + K<sub>2</sub>O, 3.62–4.70 wt%) and do not correlate with SiO<sub>2</sub>. San Jorge, however, does correlate positively with SiO<sub>2</sub> at lower total alkali content (2.64–3.08 wt%). Villarrica compositions also correlate positively with SiO<sub>2</sub> and have a greater range in total alkali content, spanning the range between the main SEC group and San Jorge. Huililco samples extend to the highest values of SiO<sub>2</sub> (Fig. 2a), and are also notably elevated in K<sub>2</sub>O (Fig. 2h). MgO values range between 4 and 8 wt% except for San Jorge, which has significantly higher MgO content (10–12 wt% MgO) at similar SiO<sub>2</sub> content to the majority of the SECs and Villarrica and has lower Al<sub>2</sub>O<sub>3</sub>, TiO<sub>2</sub> and alkali element contents (Fig. 2b, c, g and h). There is little correlation between major elements with MgO or SiO<sub>2</sub> in the SECs. Samples from La Barda and Cabargua have values which overlap in all major elements, with the exception of CaO (Fig. 2e), where La Barda samples plot somewhat higher.

Some individual SECs display intra-centre variations which are in some cases related to the type of material analysed (see Tables 1 and 2 and the electronic appendix). This is notable between the scoria and lava samples of Huililco, San Jorge and Cabargua. In Huililco, the five samples representing the initial scoria cone building phase of the eruption extend to the highest MgO values within the centre and have lower SiO<sub>2</sub>, Na<sub>2</sub>O and K<sub>2</sub>O values than the lava samples (marked in Fig. 2h). Significantly, they do not display the strong correlation between MgO and K<sub>2</sub>O that is observed in the lava samples. A difference between scoria and lava is also clearly seen in TiO<sub>2</sub> and CaO in San Jorge samples (Fig. 2c, e). A vertical trend to high MnO is formed by some Cabargua samples, and these are identified as being not only scoria samples, but scoria solely from the second cone of this small complex; these same samples also display vertical trends in Al<sub>2</sub>O<sub>3</sub> with MgO (Fig. 2b, f).

Inter-centre compositional differences are more pronounced within trace element concentrations (Fig. 3). Chromium varies between 50 and 450 ppm for the majority of rocks with the exception of San Jorge which has highly elevated concentrations (600–870 ppm, Fig. 3a). In all other trace elements San Jorge is depleted compared

to all other rocks. Huililco samples are enriched in Rb, Zr and Th in relation to the rest of the field (Fig. 3c, e, f), and often plot with Huelemolle samples (notably in Zr and Ce, Fig. 3d, e). As in the major elements, Cabargua and La Barda generally display very similar major and trace element compositions. All centres display somewhat different characteristics in Sr vs. MgO (Fig. 3b).

Primitive mantle normalised multi-element values are typical of arcs, having prominent, low Nb–Ta values, positive Ba and Sr anomalies, and negative Ti anomalies. The centres can, however, be separated into three distinct compositional groups (Fig. 4a—representative samples with similar SiO<sub>2</sub>/MgO values of c. 8 were chosen, with the exception of San Jorge (c. 5) due to its much higher MgO values): (1) San Jorge and Villarrica: have almost identical patterns, and the most pronounced fluid mobile element (FME) concentrations for Sr, K, U and Ba of all the studied rocks, however, other incompatible elements are generally depleted resulting in characteristic high K/La and very low Nb and Ta normalised abundances, (2) Cabargua and La Barda: are similarly enriched in FMEs but with less distinct depletion in other elements, resulting in a less pronounced Nb–Ta trough and K/La ratios close to 1, (3) Huelemolle and Huililco: have the most trace element enriched patterns of the three groups, with less contrast between FMEs and high field strength elements, and a much less pronounced Nb–Ta trough. The patterns of the two centres differ in K–La, where Huelemolle has K < La and Huililco has K > La.

The three groups recognised on a primitive mantle normalised multi-element plot are not observed on a chondrite normalised rare earth element (REE) plot (Fig. 4b). Huililco, Huelemolle, La Barda and Cabargua follow the same trend of general light rare earth element (LREE) enrichment, with Huelemolle having somewhat higher values and La Barda the lowest. San Jorge and Villarrica samples are less enriched in LREEs but are similar to the other centres in normalised Heavy Rare Earth Element (HREE) values. Villarrica has a small negative Eu anomaly.

### Whole rock Sr–Nd and U–Th isotopes

Sr–Nd isotope ratios (from Morgado et al. 2015 and Hickey-Vargas et al. 2002 and 2016, Table 1) in general vary over a small range: <sup>87</sup>Sr/<sup>86</sup>Sr varies between 0.70371 and 0.70406, and <sup>143</sup>Nd/<sup>144</sup>Nd varies between 0.512812 and 0.512913. Despite this, and within the reported 2SE error, the values define a triangle (Fig. 5a) in which the end points follow the same groupings as in the multielement plots: (1) most enriched Sr–Nd (San Jorge and Villarrica), (2) least enriched Sr–mid Nd (Cabargua and La Barda) and (3) least enriched Nd–mid Sr (Huililco and Huelemolle). Higher <sup>87</sup>Sr/<sup>86</sup>Sr in Villarrica, Huililco and

**Table 2** Representative whole rock major and trace element analyses (see electronic appendix for all analyses)

Volcano	San Jorge	San Jorge	San Jorge	Huelemolle	Huelemolle	Caburgua	Caburgua	Caburgua
Sample	<sup>a</sup> SJ-T-3a	SJ-B-2A	SJ-L-5	Huel-1*	Huel-2	LEM-3	<sup>a</sup> CB-9	Cab1-1*
Material	Lapilli	Bomb	Lava	Lava	Lava	Lapilli	Lapilli	Lava
SiO <sub>2</sub>	51.65	50.26	51.4	49.96	51.28	50.98	51.51	50.26
TiO <sub>2</sub>	0.721	0.518	0.554	1.106	1.107	1.149	1.123	1.116
Al <sub>2</sub> O <sub>3</sub>	14.7	13.63	14.08	17.73	16.95	19.28	18.62	17.48
Fe <sub>2</sub> O <sub>3</sub> (T)	9.68	10.28	10.14	9.88	9.4	9.68	9.24	9.57
MnO	0.164	0.158	0.156	0.156	0.158	0.178	0.18	0.149
MgO	11.17	11.76	10.83	5.66	5.57	5.31	4.89	6.8
CaO	9.96	8.98	9.2	9.4	9.43	8.89	8.71	8.68
Na <sub>2</sub> O	2.37	2.31	2.56	3.17	3.18	3.36	3.21	3.3
K <sub>2</sub> O	0.36	0.36	0.41	0.82	0.8	0.66	0.68	0.75
P <sub>2</sub> O <sub>5</sub>	0.13	0.1	0.13	0.41	0.38	0.34	0.33	0.29
LOI	0.02	-0.06	-0.33	-0.16	0.22	1.09	0.71	-0.09
Total	100.9	98.3	99.13	98.13	98.48	100.9	99.2	98.3
Na <sub>2</sub> O + K <sub>2</sub> O	2.73	2.67	2.97	3.99	3.98	4.02	3.89	4.05
Sc	33	33	33	26	26	26	26	25
V	232	228	238	224	213	238	223	229
Ba	120	118	135	305	304	301	238	266
Sr	333	328	344	593	630	720	710	798
Y	12	11	12	21	21	19	18	17
Zr	46	46	51	132	132	90	87	79
Cr	770	870	720	100	90	80	40	200
Co	46	49	46	32	32	33	34	31
Ni	220	250	210	50	50	50	30	80
Cu	70	80	80	80	80	70	60	80
Zn	70	70	80	90	80	90	80	70
Ga	16	16	16	18	18	21	16	17
Rb	7	8	8	13	13	9	9	10
Nb	1	1	1	7	5	3	2	5
Cs	0.7	0.7	0.6	0.6	0.6	0.5	0.5	0.5
La	4.6	4.6	5.3	22.7	20.5	13.4	12.6	14.4
Ce	11	10.7	12.2	48.1	45.7	31.1	30.8	31.5
Pr	1.59	1.51	1.76	5.87	5.76	4.11	3.86	4.14
Nd	7.4	7.1	8.2	24	24	17.9	17	17.6
Sm	2	1.9	2.1	5.1	5.1	4	3.7	3.9
Eu	0.72	0.67	0.77	1.49	1.51	1.21	1.25	1.2
Gd	2.2	2.3	2.3	4.7	4.6	3.6	3.2	3.8
Tb	0.4	0.4	0.4	0.7	0.7	0.5	0.6	0.6
Dy	2.3	2.2	2.5	4.2	4.1	3.3	3.4	3.2
Ho	0.5	0.5	0.5	0.8	0.8	0.7	0.7	0.6
Er	1.4	1.5	1.5	2.5	2.3	2	2	1.8
Tm	0.21	0.21	0.22	0.36	0.35	0.29	0.29	0.26
Yb	1.4	1.3	1.4	2.3	2.2	1.9	1.9	1.7
Lu	0.2	0.2	0.22	0.36	0.32	0.28	0.3	0.28
Hf	1.2	1.2	1.3	2.6	2.8	2	2	1.7
Ta	0.1	0.1	0.1	0.4	0.2	0.2	0.2	2.2
Pb	b.d.l	b.d.l	b.d.l	9	8	7	6	7
Th	0.5	0.5	0.6	2	1.7	1.9	2	2.7
U	0.4	0.3	0.3	0.6	0.6	0.6	0.6	0.7



**Table 2** continued

Volcano	Huililco	Huililco	Huililco	La Barda	La Barda	La Barda	Villarrica (2015 eruption)	Granodiorite	Granite
Sample	PVM-04	<sup>a</sup> PVM-15B	PVM-17	LEM-17	LEM-18	Barda2-3	Vill-15	LEM-7	Cord 1-1
Material	Bomb	Lapilli	Lava	Bomb	Lapilli	Lava	Spatter	Xenolith	Xenolith
SiO <sub>2</sub>	52.62	52.87	53.56	49.82	47.14	49.57	52.69	59.06	70.39
TiO <sub>2</sub>	1.08	0.945	1.162	1.058	1.129	1.108	1.241	0.59	0.408
Al <sub>2</sub> O <sub>3</sub>	16.76	16.13	17.03	17.17	18.47	16.98	16.63	17.73	14.1
Fe <sub>2</sub> O <sub>3</sub> (T)	8.89	8.7	8.63	10.13	10.21	10.14	10.05	6.83	3.62
MnO	0.15	0.146	0.145	0.154	0.159	0.155	0.165	0.113	0.073
MgO	6.28	7.27	5.43	7.34	7.57	7.14	5.74	3.15	0.89
CaO	8.69	9.02	8.9	9.34	8.25	9.42	9.35	6.49	2.16
Na <sub>2</sub> O	3.1	2.79	3.12	3.12	2.63	3.02	3.28	3.54	3.67
K <sub>2</sub> O	1.1	0.89	1.18	0.63	0.47	0.67	0.79	1.77	3.74
P <sub>2</sub> O <sub>5</sub>	0.33	0.29	0.39	0.32	0.33	0.33	0.23	0.17	0.09
LOI	-0.2	-0.19	-0.24	0.6	4.36	0.24	0.04	1.46	0.5
Total	98.81	98.86	99.31	99.66	100.7	98.76	100.2	100.9	99.64
Na <sub>2</sub> O + K <sub>2</sub> O	4.2	3.68	4.3	3.75	3.1	3.69	4.07	5.31	7.41
Sc	26	27	27	28	30	28	34	24	6
V	208	200	211	236	225	235	308	194	53
Ba	349	284	365	283	200	247	239	795	693
Sr	547	502	572	689	601	683	433	551	226
Y	20	18	23	16	17	18	25	19	14
Zr	130	107	137	86	96	91	107	74	182
Cr	190	300	130	290	260	190	150	30	<20
Co	35	37	31	33	36	32	33	16	5
Ni	90	130	50	80	80	70	80	20	<20
Cu	70	60	60	90	70	70	160	60	120
Zn	90	70	70	80	80	70	90	90	40
Ga	14	13	13	18	19	17	19	20	14
Rb	28	22	30	9	6	9	20	55	116
Nb	7	4	9	3	3	3	2	4	5
Cs	1.2	1.1	1.3	0.5	0.5	0.5	2	2.5	2.6
La	17.4	14.1	18.4	13.6	14.8	15.5	10.1	13.7	16
Ce	40.2	32.3	41.5	30.3	31.8	32.9	24.8	29.3	31.2
Pr	4.99	4.09	5.2	4.13	4.36	4.21	3.52	3.84	3.64
Nd	19.9	16.8	20.7	17.7	19.2	17.8	16.3	16.5	13.5
Sm	4.3	3.6	4.3	4	4.1	4	4.2	3.9	2.8
Eu	1.37	1.26	1.43	1.23	1.33	1.27	1.27	0.98	0.68
Gd	3.7	3.3	3.9	3.8	4.1	3.9	4.7	3.8	2.5
Tb	0.6	0.6	0.7	0.6	0.6	0.6	0.8	0.6	0.4
Dy	4	3.6	3.9	3.3	3.6	3.4	4.9	3.5	2.3
Ho	0.8	0.7	0.8	0.7	0.7	0.7	1	0.7	0.5
Er	2.2	2	2.3	2	2.2	2	2.9	2.1	1.5
Tm	0.32	0.29	0.33	0.29	0.32	0.29	0.41	0.32	0.23
Yb	2.1	1.9	2.1	1.9	2.1	1.8	2.7	2	1.7
Lu	0.33	0.32	0.34	0.29	0.32	0.29	0.41	0.3	0.32
Hf	3	2.4	3.2	2.2	2.4	1.9	2.7	2.1	4
Ta	0.5	0.3	0.6	0.2	0.2	0.1	0.1	0.2	9.6
Pb	8	6	7	6	7	7	9	7	14
Th	3.4	2.6	3.5	2	2.2	2.1	1.5	3.5	11.1
U	1	0.8	1	0.7	0.7	0.6	0.6	1	3.3

\*Reported in Morgado et al. (2015)

<sup>a</sup> Olivine and olivine-hosted melt inclusion analyses for these samples (Table 4)

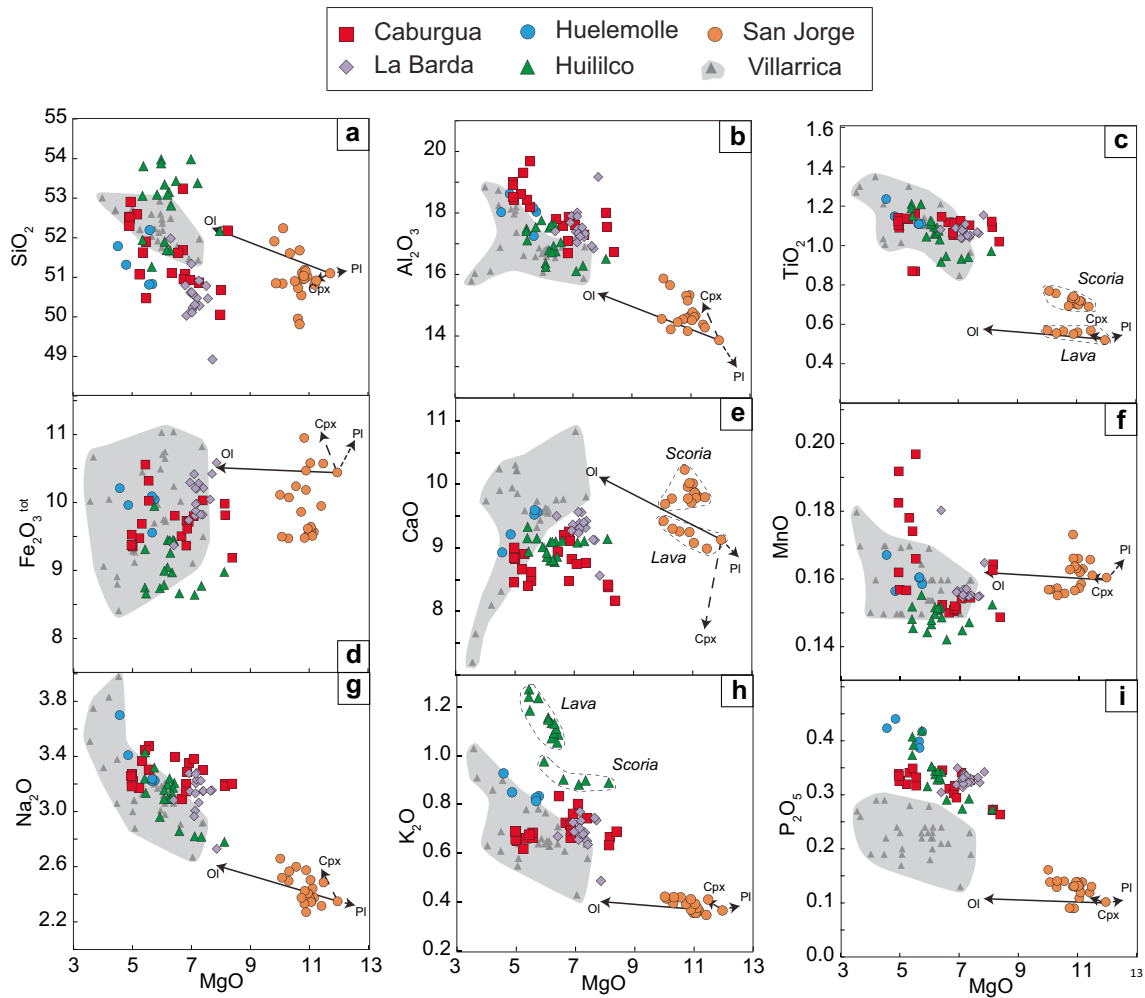


**Fig. 2** Major element compositions in wt% for the Pucón SECs and Villarrica. Villarrica data are from Hickey-Vargas et al. (1989), Morgado et al. (2015) and Wehrmann et al. (2014). Dashed lines surround samples from particular phases of certain eruptions, as discussed in the text. Mineral vectors are mass balance calculations using analy-

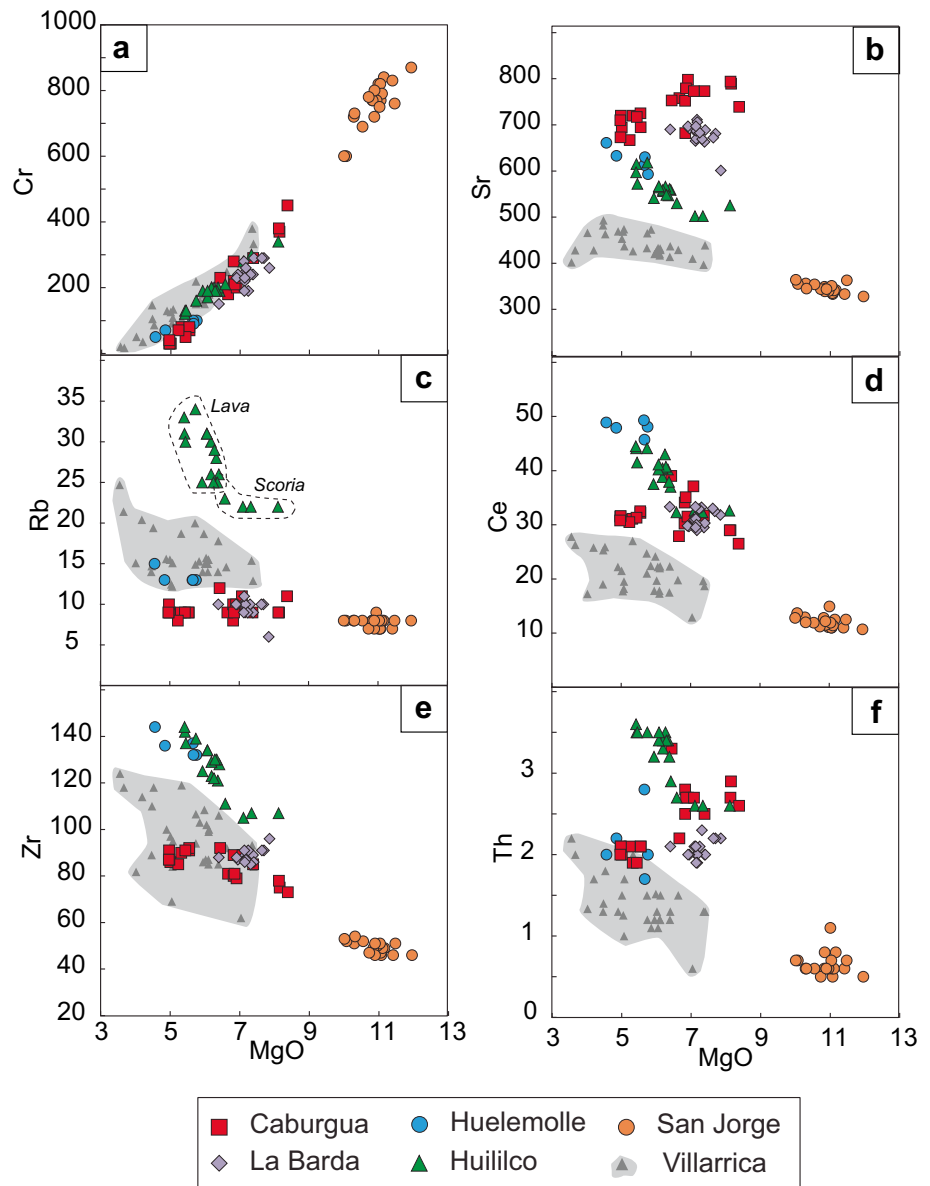
ses of clinopyroxene (Cpx, line represents 10% crystallisation), plagioclase (Pl, line represents 5% crystallisation) and olivine (Ol, line represents 10% crystallisation) from San Jorge lava from Morgado et al. (2015)

two Huelemolle samples is accompanied with higher  $\text{SiO}_2$  (also from the above data sources); this is not observed in the higher  $^{87}\text{Sr}/^{86}\text{Sr}$  of San Jorge (Fig. 5b).

U-Th isotopic analyses for the Pucón SECs and Villarrica (Fig. 5c; Table 3, standard data are presented in the electronic appendix) lie in fields of Uranium- (U-) excess (San Jorge and Villarrica), on the equiline (Huililco and Huelemolle and some La Barda samples) and Thorium- (Th-) excess (Caburgua and some La Barda). San Jorge samples have higher  $(^{238}\text{U}/^{232}\text{Th})$  ratios than Villarrica (parentheses denote activity ratios): 1.136–1.290, which are the highest thus far reported from the CSVZ of the Southern Andes (Fig. 5c), and additionally lie outside the general field of arc rocks of Lundstrom (2003).  $(^{238}\text{U}/^{232}\text{Th})$  ratios between the SECs Huelemolle,

Caburgua, La Barda and Huililco occupy a narrow range: 0.842–0.955.  $(^{230}\text{Th}/^{232}\text{Th})$  is more variable within these centres, ranging from 0.867 in Huililco to 0.964 in Huelemolle. Individual SECs plot in their own groups, with no overlap between centres, with the exception of one sample each from La Barda and Caburgua. There is a negative trend from La Barda and Caburgua to Huililco, San Jorge and Villarrica trend in  $^{87}\text{Sr}/^{86}\text{Sr}$  vs.  $(^{230}\text{Th}/^{232}\text{Th})$ , with the exception of Huelemolle which lies at higher  $(^{230}\text{Th}/^{232}\text{Th})$  (Fig. 5e). In  $^{87}\text{Sr}/^{86}\text{Sr}$  vs.  $(^{238}\text{U}/^{230}\text{Th})$ , however, San Jorge and Villarrica samples have high U-excesses at similar  $^{87}\text{Sr}/^{86}\text{Sr}$  to Huelemolle and Huililco, which lie in secular equilibrium, whilst Caburgua and La Barda samples are partially into the Th-excess field at slightly lower  $^{87}\text{Sr}/^{86}\text{Sr}$  (Fig. 5f).

**Fig. 3** Selected trace element concentrations in ppm plotted against MgO in wt%. Villarrica data sources are as in Fig. 2 and Table 1



### Olivine and olivine-hosted melt inclusion analyses

Representative melt inclusion data are shown in Table 4, all data (including host olivine) and standards are presented in the electronic appendix. Ranges of Fo# (forsterite) olivine Fo# and whole rock Mg# (magnesium number) are calculated as  $[\text{Mg}/\text{Mg} + \text{Fe}] \times 100$  for the three samples studied are as follows: Caburgua 78–82, Huililco 77–87 and San Jorge 85–89. Using the  $\text{KD}^{\text{Fe-Mg}}$  values of Roeder and Emslie (1970), Caburgua olivines are within equilibrium with their host rock Mg# (55), some Huililco olivines are within equilibrium but the majority have too low Fo# for their host rock Mg# (66), whilst all San Jorge olivines plot slightly below equilibrium (host rock Mg#: 73). Melt inclusions from all three samples are in equilibrium with their

host olivines once corrected for post entrapment crystallisation (PEC) (Fig. 6a). We note that correction for PEC does not affect the minor elements and ratios that are used in this study.

Melt inclusions within olivines from the chosen three samples (see Table 1) were analysed for their major element (in wt%), S and Cl (reported in ppm) contents. The three samples form distinct groups in almost all melt inclusion compositions (Fig. 6). Note that comparative fields from the literature plotted in Fig. 6 are for melt inclusion data only.  $\text{SiO}_2$  contents for Caburgua and San Jorge melt inclusions are lower than the plotted whole rock data for each volcano, whilst  $\text{K}_2\text{O}$  values overlap within each centres data (Fig. 6b). This is due to olivine crystallisation, as shown by model lines in Fig. 6b. In contrast, Huililco

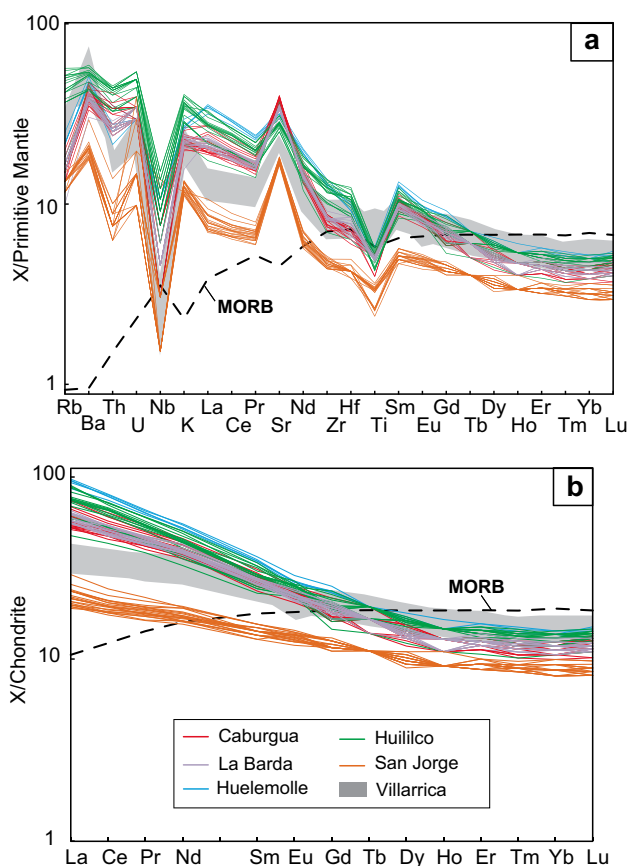


**Fig. 4** **a** Primitive mantle normalised (after Sun and McDonough 1989) multi-element plot and **b** Chondrite normalised (after McDonough and Sun 1995) REE plot. Mid Ocean Ridge Basalt is plotted on each from McDonough and Sun, 1995. All samples from the small eruptive centres are plotted, and Villarrica data from Morgado et al. (2015), Wehrmann et al. (2014) and the 2015 sample from this study are plotted as a grey field

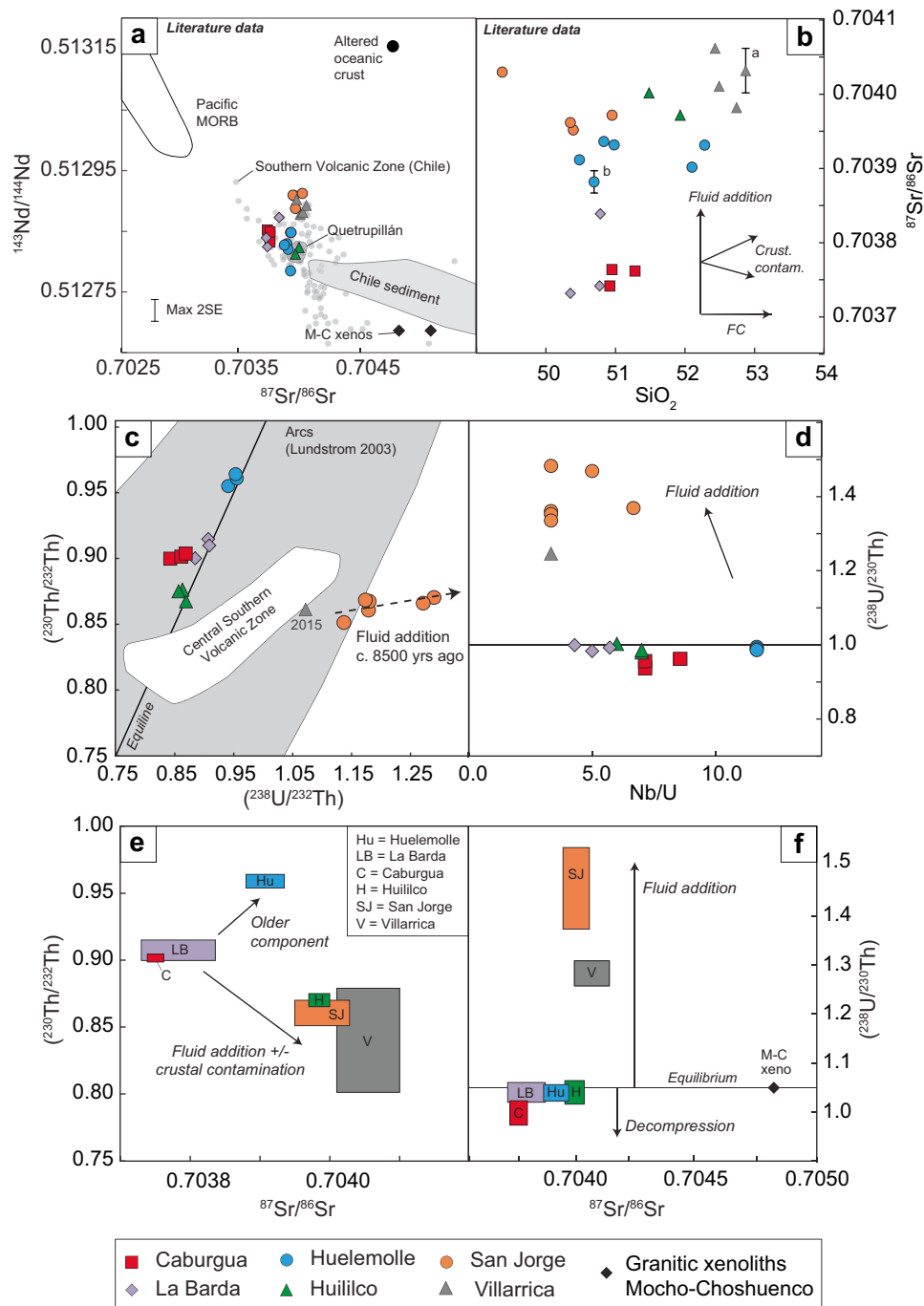
inclusions  $\text{SiO}_2$  and  $\text{K}_2\text{O}$  values overlap with those of the whole rock.  $\text{TiO}_2$  values for Caburgua inclusions are slightly lower than whole rock values, whereas in Huililco inclusions have higher  $\text{TiO}_2$  than whole rock values. San Jorge inclusions overlap in  $\text{TiO}_2$  with whole rock values from the explosive phase only. Literature MI data from Villarrica (Wehrmann et al. 2014) form two groups: one similar to whole rock values, the other trending to higher  $\text{SiO}_2$ ,  $\text{K}_2\text{O}$  and  $\text{TiO}_2$ , as in Huililco. In volatile content, all three centres exhibit relatively high S contents (960–2260 ppm, similar to other CSVZ monogenetic centres, Fig. 6e) with Caburgua standing out at the highest values (1337–2260 ppm). Caburgua and Huililco display similar values of Cl (c. 700 ppm) whilst San Jorge lies at lower values (c. 500 ppm). Cl values are lower than those found in olivine-hosted melt inclusions for Volcán Apagado and Cabeza de Vaca (the former is a scoria cone with evidence of multiple eruption phases, and the latter is a truly monogenetic

**Fig. 5** Whole rock isotopic data. **a** Sr–Nd isotopes from Morgado et al. (2015) and Hickey-Vargas et al. (1989) and 2016 for the Pucón area (see Table 1). Southern Volcanic Zone (Chile) analyses were compiled from the Georoc database, filtered for  $\text{MgO}$  4.5–12 wt%. ‘Pacific MORB’ is Pacific Mid Ocean Ridge Basalt (from a compilation by Stracke et al. 2003). ‘Chile sediment’ is trench sediment from Lucasen et al. (2010). ‘M-C xenos’ are partially melted upper crustal granites from within lavas of Mocho-Choshuenco volcano 60 km south of Villarrica (McMillan et al. 1989), see Fig. 1a. Altered oceanic crust is from Jacques et al. (2014). **b** variation in  $^{87}\text{Sr}/^{86}\text{Sr}$  with  $\text{SiO}_2$  for the same samples as in (a). The 2SE error bar marked ‘a’ is for Huililco and Villarrica data (Hickey-Vargas et al. 1989) and the smaller 2SE error bar marked ‘b’ is for all other data; the annotated lines show possible explanations for the trends, which are discussed in the text. **c** U–Th isotopic data from this study; note that the Villarrica analysis is for a sample erupted in 2015. The CSVZ (Central Southern Volcanic Zone) data (excluding the stratovolcano Osorno, which lies at much lower  $(^{230}\text{Th}/^{232}\text{Th})$ , 0.72) are from Jicha et al. (2007), Reubi et al. (2011) and Sigmarsson et al. (2002), and the grey field represents U–Th isotopic data for arc volcanoes from Lundstrom (2003). The isochron of possible fluid addition was calculated using the formula  $(-1/\lambda^{230}\text{Th}) \times \text{Ln}(1-m)$ , where  $\lambda^{230}\text{Th}$  is taken as  $9.171\text{E}-6$  (using the half-life of  $^{230}\text{Th}$  of Cheng et al. 2013) and  $m$  is the slope of the isochron, in this case 0.0754. **d** Shows elevated  $(^{238}\text{U}/^{232}\text{Th})$  at similar Nb/U for San Jorge and Villarrica samples. **e** Shows the correlation between  $(^{230}\text{Th}/^{232}\text{Th})$  and Sr isotopes, **f** shows the correlation between U-excess and Sr isotopes and the influence of fluid input. In **e** and **f** the maximum range is shown for each sample as U–Th isotopes are from this study and Sr isotopes are from the literature (see Table 1) on different samples. Note also that **e** and **f** Villarrica data include two samples from the 1984 and 1971 eruptions from Sigmarsson et al. (2002) which are within the CSVZ field in **e**

volcano; note that these are labelled ‘CSVZ monogenetic’ on Fig. 6 as they are labelled thus in their respective data sources) at 1057–1637 ppm (Wehrmann et al. 2014). Analyses from the present study form a curved negative trend in  $\text{Cl}/\text{K}$  vs.  $\text{K}_2\text{O}/\text{TiO}_2$ , from San Jorge at the highest  $\text{Cl}/\text{K}$  to Huililco at the lowest and with the greatest range in  $\text{K}_2\text{O}/\text{TiO}_2$  ratios (Fig. 6d, e). As in the major elements, literature volatile data for Villarrica melt inclusions form two groups: one which follows the trend of the SEC data, and one with a steeper decrease in  $\text{Cl}/\text{K}$  over  $\text{K}_2\text{O}/\text{TiO}_2$ .

## Discussion

When compositions of the SECs and nearby stratovolcanoes in the Pucón area are plotted with longitude it can be seen that heterogeneity cannot be correlated with distance from the arc front (Fig. 7). This conflicts with the findings of Watt et al. (2013) who suggested that in strato- and monogenetic volcanoes further into southern Chile (at  $42^\circ\text{S}$  and  $44^\circ\text{S}$ )  $\text{K}_2\text{O}$  and  $\text{MgO}$  contents increase with distance from the arc front, and degrees of melting decrease as slab-released water becomes less dominant in the melting regime. The Pucón area is complex in that it contains an arc-scale fault (the LOFS) in addition to the scatter of SECs amongst stratovolcanoes in a



NW-aligned chain related to inherited basement features (Moreno and Clavero 2006; Cembrano and Lara 2009), the latter representing longer lived magmatic systems and therefore more complicated plumbing systems (Fig. 1). Simple size- or location-related conclusions cannot be drawn from the data; for example,  $^{87}\text{Sr}/^{86}\text{Sr}$  (highest in Villarrica, Quetrupillán, Huililco and San Jorge) cannot be correlated with  $\text{K}_2\text{O}$  (used as a proxy for crustal contamination, and highest in Quetrupillán and Huililco,

lowest in San Jorge) or  $\text{K}/\text{La}$  (used as a proxy for slab fluid input due to the mobility of K over La, and highest in Villarrica, Quetrupillán and San Jorge, lowest in Huelemolle). U-excess is roughly correlated with  $\text{K}/\text{La}$  (both are highest in Villarrica and San Jorge, Fig. 7), suggesting a similar fluid component for these centres despite their disparity in size (see later discussion). It is clear that the LOFS-aligned SECs have some geochemical characteristics distinct from isolated SECs and the stratovolcanoes

**Table 3** U-Th isotopic analyses for selected Pucón SECs and the 2015 eruption of Villarrica

Volcano	Sample	$(^{238}\text{U}/^{232}\text{Th})$	$(^{230}\text{Th}/^{232}\text{Th})$	$(^{238}\text{U}/^{230}\text{Th})$
San Jorge	SJ-B-2A	1.290	0.870 ± 1	1.482 ± 3
San Jorge	SJ-T-3	1.271	0.866 ± 2	1.468 ± 3
San Jorge	SJ-T-6	1.178	0.861 ± 2	1.368 ± 4
San Jorge	SJ-L-1	1.180	0.868 ± 2	1.360 ± 3
San Jorge	SJ-L-3	1.174	0.868 ± 2	1.352 ± 3
San Jorge	SJ-L-6	1.136	0.851 ± 2	1.334 ± 4
Huelemolle	Huel-1	0.955 ± 1	0.961 ± 1	0.994 ± 2
Huelemolle	Huel-3	0.953 ± 1	0.964 ± 2	0.989 ± 3
Huelemolle	Huel-6	0.941 ± 1	0.955 ± 2	0.985 ± 3
Caburgua	Cab1-1	0.842	0.900 ± 2	0.936 ± 3
Caburgua	Cab2-1	0.869 ± 1	0.904 ± 3	0.961 ± 3
Caburgua	Cab3-1	0.861 ± 1	0.901 ± 2	0.955 ± 3
Huililco	LEM-10	0.869	0.867 ± 1	1.002 ± 2
Huililco	PVM-04	0.856	0.875 ± 2	0.979 ± 2
Huililco	PVM-06	0.863	0.876 ± 2	0.985 ± 3
La Barda	LEM-19	0.908	0.910 ± 2	1.000 ± 2
La Barda	LEM-24	0.907 ± 1	0.915 ± 2	0.990 ± 2
La Barda	Barda1-2	0.884 ± 1	0.900 ± 2	0.982 ± 3
Villarrica (2015 eruption)	Vill-15	1.072 ± 1	0.861 ± 1	1.245 ± 3

Errors are 2SE ( $^{238}\text{U}/^{232}\text{Th}$ ) analyses with no error listed had 2SE < 0.001)

(higher sulphur in melt inclusions from Caburgua, lower  $^{87}\text{Sr}/^{86}\text{Sr}$  in Caburgua and La Barda Fig. 7) suggesting that these may be related to their tectonic context. These brief conclusions alone show the competing dominance of magmatic and tectonic processes in producing compositional heterogeneity, the lack of trend with increasing distance from the slab (as evidenced by the large contrast between Huililco and San Jorge samples, Fig. 7), and importantly, the clear isolation of subsequent evolution of individual melt batches despite the volcanic centres' close proximity in space and time (as also noted by Watt et al. 2013).

Great heterogeneity is observed in the SECs of the Pucón area which highlight the variation in aspects of magma genesis and processing within this small area. Figure 8 shows examples of geochemical parameters where compositions from different SECs lie on different trajectories which are related to components in the system and cannot be linked by mixing between the groups, or by one process (such as melting). The following discussion uses the powerful combination of U-series isotopes, olivine-hosted melt inclusions and major and trace element models to elucidate details of the magma plumbing system in Pucón and its connection to the active arc and tectonic features in the area.

## Deep processes

### *Two distinct source compositions are identified through U-series and trace element systematics*

The fact that the three samples analysed for olivine-hosted melt inclusions plot as three distinct fields (Fig. 6) shows the generation of three distinct melts, and thus the isolation of each melting event. Two patterns only, however, are observed in chondrite normalised-REE concentrations: a near flat pattern where LREE concentrations are only slightly higher than HREE concentrations (San Jorge and Villarrica), and a pattern at similar middle- and HREE concentrations as San Jorge but with comparatively higher concentrations of LREE (La Barda, Caburgua, Huililco and Huelemolle, with Huelemolle lavas extending to the highest La and Ce values) (Fig. 4b). These characteristics are indicative of a similar source for both groups melted to different degrees (affecting mainly the LREE). However, other parameters, such as the generally lower trace element content (Figs. 3, 4), lower whole rock  $\text{Al}_2\text{O}_3$  and whole rock and melt inclusions  $\text{TiO}_2$  (Figs. 2, 6), suggest that the San Jorge source is more depleted—or has been subjected to previous melt extraction—compared to the source of the other SECs. This is corroborated by the distinctly different trend in  $\text{Dy}/\text{Dy}^*$  vs.  $\text{Dy}/\text{Yb}$  space, with San Jorge and Villarrica samples shifted in the direction of a LREE-depleted source (Fig. 8a), their offset from the main trend in Sr–Nd space (Fig. 5a) and the two broad groups of data in U–Th space (Fig. 5c, d).

Figure 9 shows modelled melt compositions for three possible sources (all parameters are given in the electronic appendix). The models show that melting of a primitive mantle composition (Hofmann 1988) containing 4% modal spinel creates a pattern with too little contrast between LREE and HREE for the majority of the SECs (Fig. 9a). This problem is also encountered when a depleted composition based on primitive mantle is used, and the pattern is highly dissimilar to all SECs with the exception of San Jorge. Clearly, a component containing garnet is required to melt in small proportions in order to explain the slight depletion in HREE which cannot be achieved with purely a spinel-bearing source. A garnet-bearing source on its own cannot be a viable possibility as its presence depletes the HREE more than is observed in our dataset (Fig. 9a). Therefore, we model the source as being a mixture between small-degree melts of a garnet-bearing source and larger-degree melts of a somewhat depleted spinel-bearing source (Fig. 9b). The proportion of garnet source is always very small (no greater than 20%). This indicates that melting begins deep in all cases, and progresses upwards where more substantial melting

**Table 4** Representative normalised anhydrous olivine-hosted melt inclusion analyses from three Pucón SEC samples. All analyses are in wt% except for Cl and S which are in ppm. All analyses including host olivines are presented in the electronic appendix

Volcano/sample	San Jorge (sample SJ-T-3a)				Caburgua (sample LEM-CB-9)			
	SJ-T-3a-15	SJ-T-3a-8	SJ-T-3a-2	SJ-T-3a-5	CB-9-1	CB-9-6	CB-9-12	CB-9-17
SiO <sub>2</sub>	45.49	45.68	49.63	49.22	47.93	47.83	47.32	46.64
TiO <sub>2</sub>	0.60	0.70	0.75	0.74	1.01	1.17	1.08	1.05
Al <sub>2</sub> O <sub>3</sub>	12.76	14.00	15.40	15.27	16.39	16.72	16.65	16.11
FeO	14.18	11.74	9.35	9.09	12.89	12.01	11.58	14.06
Fe <sub>2</sub> O <sub>3</sub>	1.75	1.45	1.15	1.12	1.59	1.48	1.43	1.74
MgO	14.16	14.23	10.29	11.16	7.59	7.63	8.58	8.59
MnO	0.19	0.17	0.18	0.16	0.24	0.20	0.17	0.24
CaO	8.62	9.42	10.24	10.43	8.12	7.90	8.59	7.43
K <sub>2</sub> O	0.27	0.31	0.39	0.32	0.77	0.86	0.79	0.79
Na <sub>2</sub> O	1.88	2.14	2.44	2.32	3.03	3.65	3.33	2.89
P <sub>2</sub> O <sub>5</sub>	0.10	0.08	0.13	0.11	0.36	0.37	0.35	0.34
Cl (ppm)	424	506	538	550	746	915	853	730
S (ppm)	1122	1647	1119	1119	1720	2260	1858	2176
Total	100	100	100	100	100	100	100	100
Sample	Huillilco (sample PVM-15b)							
Inclusion	PVM-15b-3	PVM-15b-7	PVM-15b_n_3		PVM-15b_n_15		PVM-15b_n_12	
SiO <sub>2</sub>	50.78	49.28	51.04		55.36		52.72	
TiO <sub>2</sub>	1.30	1.20	1.17		1.37		1.24	
Al <sub>2</sub> O <sub>3</sub>	14.88	15.17	18.53		15.97		15.97	
FeO	11.26	12.77	6.24		7.51		9.00	
Fe <sub>2</sub> O <sub>3</sub>	1.39	1.58	0.77		0.93		1.11	
MgO	7.58	7.44	6.94		5.21		5.86	
MnO	0.22	0.23	0.11		0.15		0.17	
CaO	7.37	7.35	10.98		7.79		8.85	
K <sub>2</sub> O	1.15	1.12	0.71		1.34		1.07	
Na <sub>2</sub> O	3.62	3.49	3.05		3.86		3.49	
P <sub>2</sub> O <sub>5</sub>	0.38	0.35	0.34		0.40		0.43	
Cl (ppm)	832	734	738		904		831	
S (ppm)	1209	1260	1260		1126		1085	
Total	100	100	100		100		100	

occurs. The sources and the potential mixing are shown in  $(La/Yb)_N$  vs.  $(Gd/Yb)_N$  ratio modelling (Fig. 8b), although the trace element depletion in San Jorge rocks suggests that its mantle source is more depleted than that of the other SECs. While the melting and minor incorporation of a source containing garnet could explain the presence of small <sup>230</sup>Th-excesses (Fig. 5c) as Th is more incompatible than U in garnet-bearing assemblages and thus concentrates in the melt, there are other means of generating such excesses which must be considered such as decompression melting, which could be related to the position of the SECs with Th-excess over the LOFS (e.g. Bucchi et al. 2015; Hickey-Vargas et al. 2016; Lara et al.

2006), and dilution of U-excesses by assimilation of crustal rock types (c.f. Jicha et al. 2007; Reubi et al. 2011) (see later sections).

A depleted source such as that modelled in Fig. 9b would not require such high degrees of melting for San Jorge as have previously been suggested by Hickey-Vargas et al. (2016) and Sun (2001) to explain the observed  $(La/Yb)_N$  and  $(Gd/Yb)_N$  ratios, which is far more in-keeping with the monogenetic nature of this SEC (e.g. McGee and Smith 2016). However, we suggest that San Jorge was affected by greater degrees of melting than the other SECs due to a large fluid influence to the source, for which there is abundant evidence.

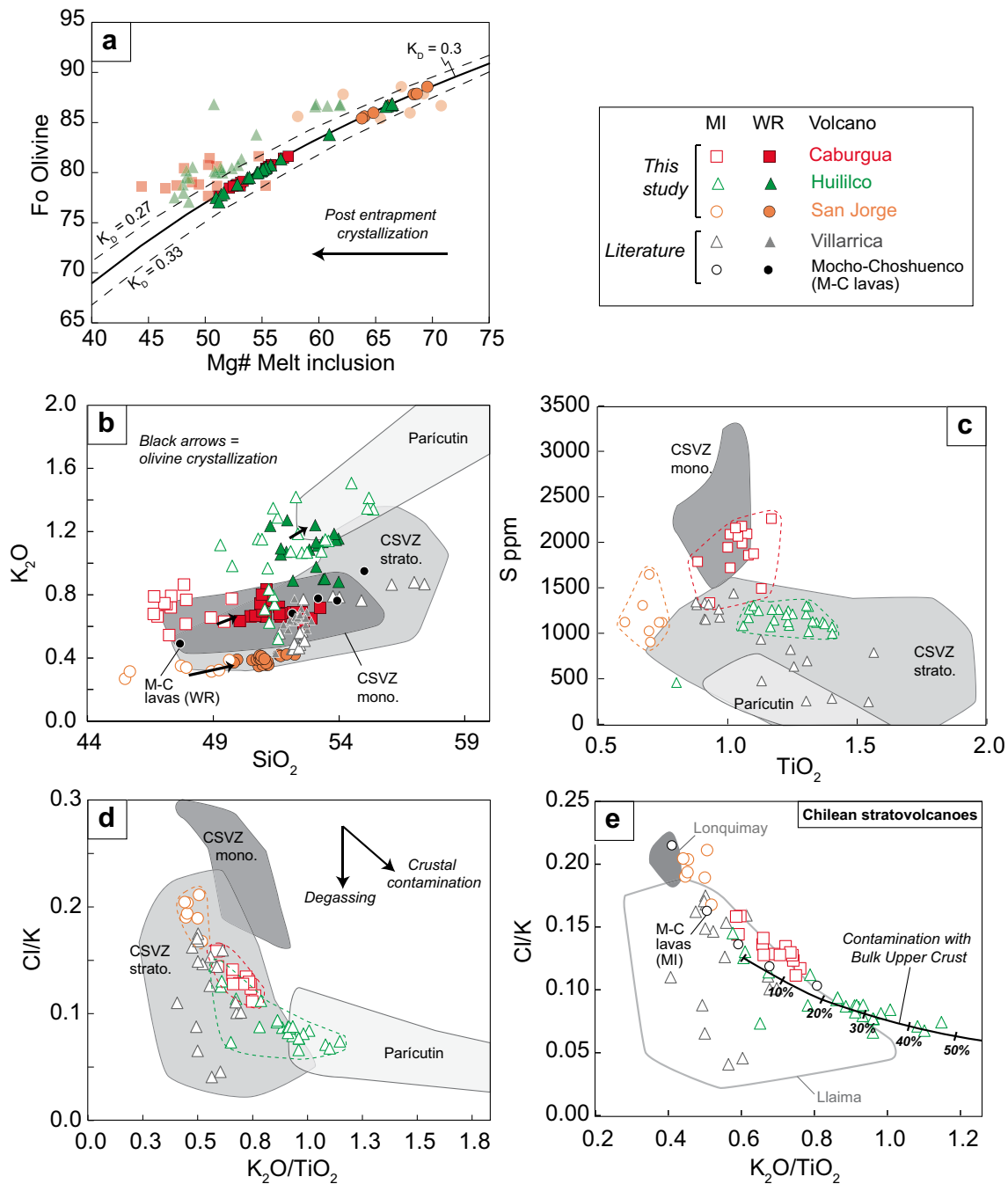


**Fig. 6** **a** Host olivine Fo vs. melt inclusion Mg# for San Jorge, Caburgua and Huililco samples. Data corrected for post entrapment crystallisation (PEC) (after Rowe et al. 2011a) are shown as filled symbols, transparent symbols are before PEC correction. All points after PEC are in equilibrium of  $K_D$  0.3 (Roeder and Emslie 1970). **b–e** Whole rock (WR) and melt inclusion (MI) major and trace element and volatile data for the three small eruptive centres compared to Villarrica WR data (Hickey-Vargas 1989 and Morgado et al. 2015), Villarrica MI data (Wehrmann et al. 2014), and literature MI data for other CSVZ monogenetic volcanoes ('CSVZ mono.') and stratovolcanoes ('CSVZ strato.') (compiled from Bouvet de Maisonneuve et al. 2012; Watt et al. 2013; Wehrmann et al. 2014) and Paricutin (Rowe et al. 2011b), the latter being the classic case study of crustal assimilation prior to olivine crystallisation in a small eruptive centre. WR

data for the Mocho-Choshuenco lavas (McMillan et al. 1989) are also plotted in (b) to show the validity of crustal assimilation at Huililco. The black arrows in (b) show olivine crystallisation for each sample, using the program COMAGMAT, assuming an anhydrous system and an oxygen fugacity of QFM, and plotting the liquid composition before the appearance of plagioclase or clinopyroxene. **e** Is a close-up version of (d) showing CSVZ MIs for specific volcanoes (references as above), and discussed in detail in the main text. Contamination is simply modelled as a straight A + B mixture using the upper crust average value (Cl: 0.037 ppm,  $K_2O$ : 2.8 wt%,  $TiO_2$ : 0.64 wt%) from Rudnick and Gao (2004) using a Huililco melt inclusion with one of the highest Cl/K values (marked in the electronic appendix). See text for discussion and Fig. 1a for stratovolcano locations



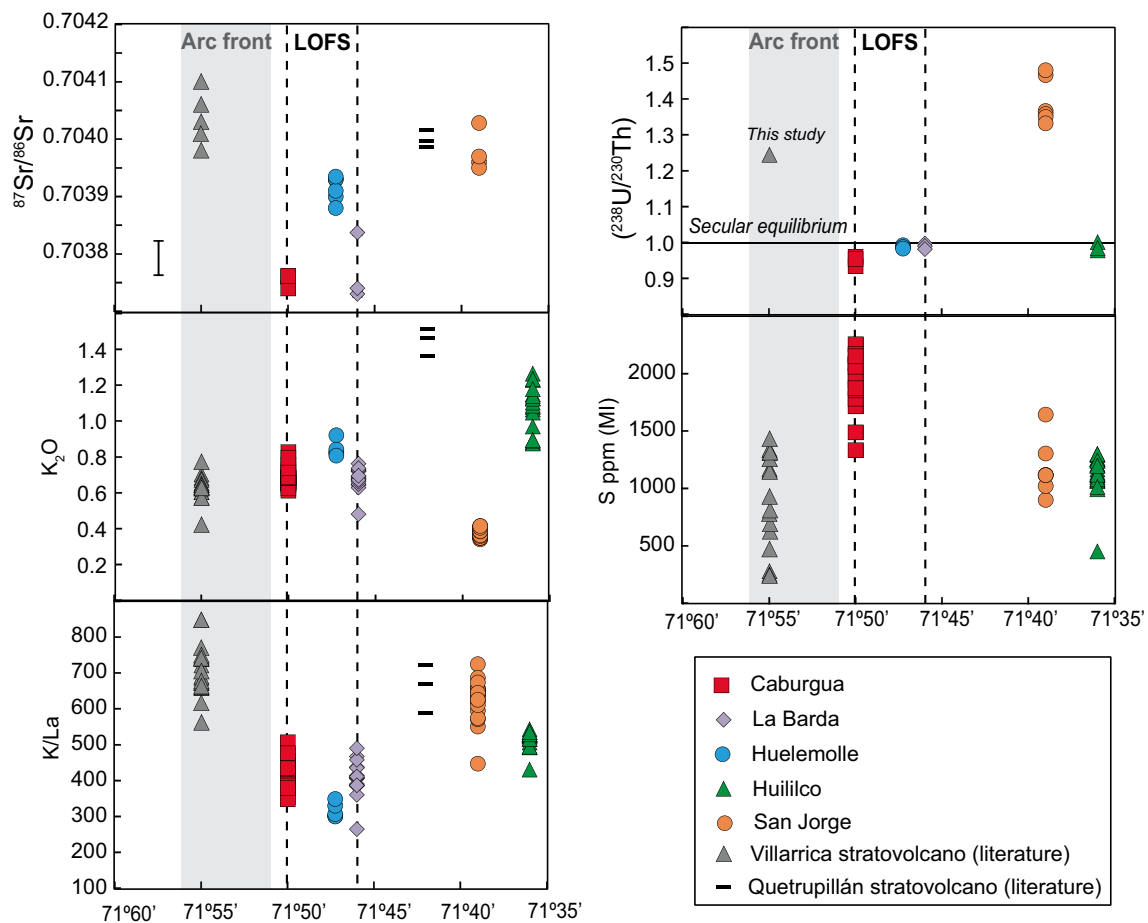


**Fig. 7** Variation in compositional parameters with longitude, or distance from the arc front (see Fig. 1b). Villarrica whole rock data sources are as in Fig. 2, Quetrupillán whole rock data are from Hickey-Vargas et al. (1989). Villarrica melt inclusion sulphur data are from Wehrmann et al. (2014). Neither  $^{87}\text{Sr}/^{86}\text{Sr}$  nor  $(^{238}\text{U}/^{230}\text{Th})$  can be correlated with  $\text{K}_2\text{O}$  (used as a proxy for crustal contamination) or

$\text{K}/\text{La}$  (used as a proxy for slab fluid input) highlighting the complexity of the compositional heterogeneity in this small area. The similarity of Caburgua and La Barda compositions and their position on the Liquiñe Ofqui fault system (LOFS) suggests a structural/tectonic control in some SECs

#### *Timing of fluid enrichment of the source in Southern Chile is seen through U-Th isotopes*

The San Jorge samples are marked by their low  $\text{TiO}_2$  (Fig. 2c), depleted trace element content, large contrast between FMEs and High Field Strength Elements (HFSEs) (Fig. 4), high Cr (Fig. 3a) and comparatively high U-excess (Fig. 5c–e). These characteristics are similar to those that mark boninites (e.g. Arndt 2003; Cameron et al. 1983; Stern et al. 1991), although San Jorge rocks are not classed as boninitic as they do not extend to high enough  $\text{SiO}_2$  or sufficiently low  $\text{TiO}_2$ , and do not contain orthopyroxene (see references above for a discussion of these characteristics). Their similarity, however, may help in elucidating their petrogenesis. It has already been shown in the modelling in Fig. 9 that these melts were produced from a depleted mantle, which we suggest had seen prior melt

extraction compared to the sources of the other SECs. It is likely that this depleted source region was highly altered by fluids from the down-going slab. Fluid enrichment in San Jorge magmas is supported by elevated Ba/Th and K/La ratios compared to the other SECs (Fig. 8c). Although it has recently been shown that U-excess is not necessarily caused by fluid input to the source region and that it can in some cases be attributed to mantle in-growth and crustal input (Huang et al. 2016), high  $^{87}\text{Sr}/^{86}\text{Sr}$  observed in San Jorge samples correlating with high ratios of fluid immobile/fluid mobile elements such as Nb/U and elevated  $(^{238}\text{U}/^{230}\text{Th})$  (Fig. 5d) provides clear evidence of this. San Jorge melt inclusions have some similarities with those from volatile-rich Tongan basalts in terms of their S,  $\text{K}_2\text{O}$  and  $\text{TiO}_2$  contents, although Cl concentrations are much higher in the Tongan basalts (up to c.1000 ppm, Cooper et al. 2010). They also have similarities to Izu-Mariana arc

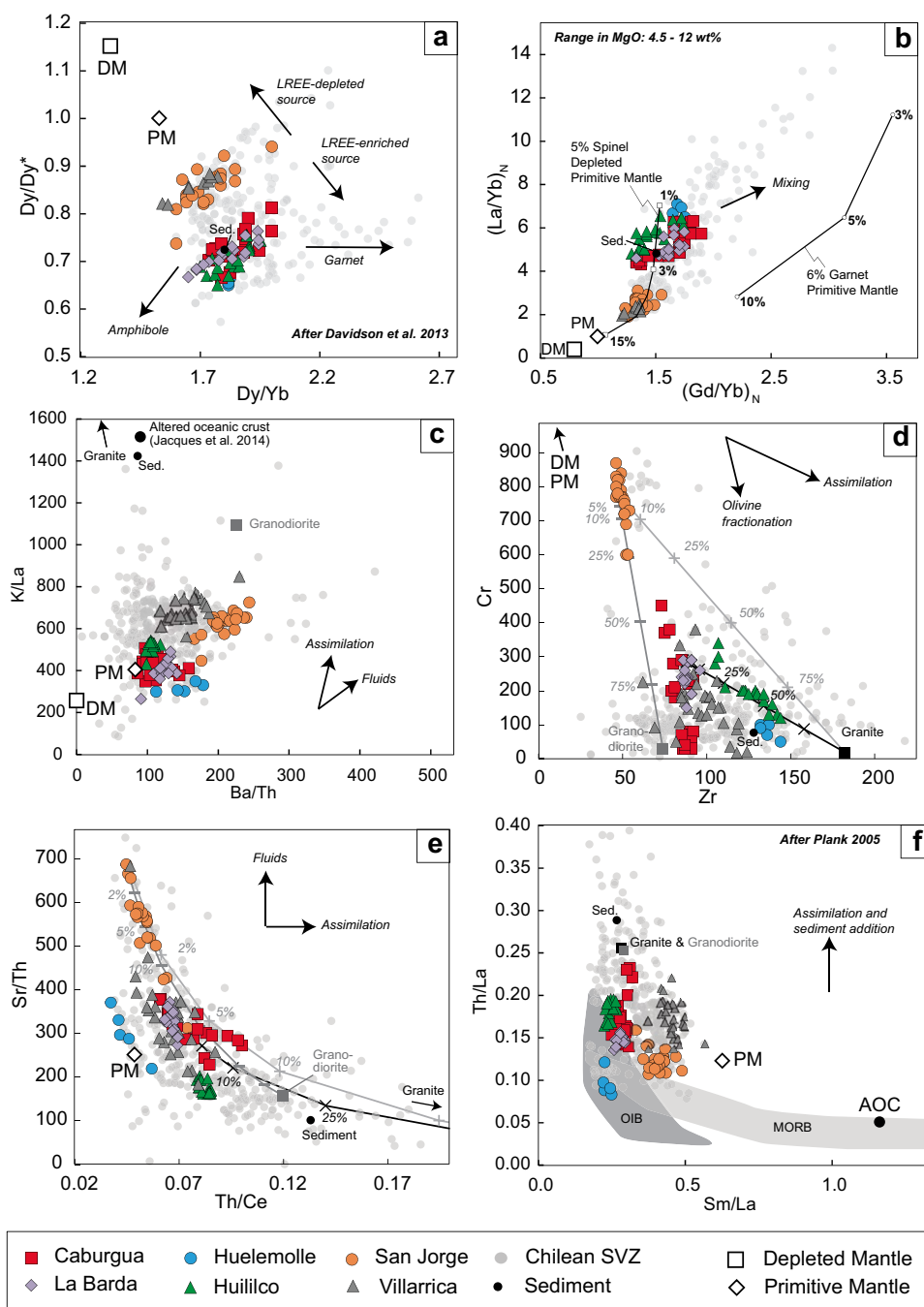


**Fig. 8** Trace element and ratio plots of the Pucon area compared to data from Georoc for the Chilean SVZ (filtered for MgO 4.5–12 wt%). Primitive and depleted mantle values are plotted or indicated for reference, and are from Sun and McDonough (1989) and Salters and Stracke (2004), respectively. AOC is the Altered Oceanic Crust value of Jacques et al. (2014), and ‘Sed.’ is trench sediment sample 97KD at latitude 39°53S from Lucassen et al. (2010). **a** and **b** show the difference in source between San Jorge and Villarrica and the other SECs;  $Dy/Dy^*$  in (**a**) is calculated from Davidson et al. (2013). In (**b**)  $(La/Yb)_N$  vs.  $(Gd/Yb)_N$  are normalised to primitive mantle values of Sun and McDonough (1989) and models of melting of garnet- and spinel-bearing sources from Fig. 9 are shown (see elec-

tronic appendix for parameters). **d** and **e** Modelling of end member components involved in the melting scenario in the Pucón area, using compositions of granite and granodiorite xenoliths found within the volcanic deposits (part of the Patagonian Batholith, see Sect. 2 and compositions in Table 2). Villarrica data sources are as in Fig. 2. **d** Cr vs. Zr discriminates between olivine fractionation and crustal assimilation. The *two lines* leading from the granite xenolith composition have different starting compositions (one San Jorge-like, the other La Barda-like). Huililco and some Villarrica trends can be reproduced by assimilation of granite starting from a La Barda-like composition. **f** Th/La vs. Sm/La is used as a discriminator for addition of sediments after Plank (2005)

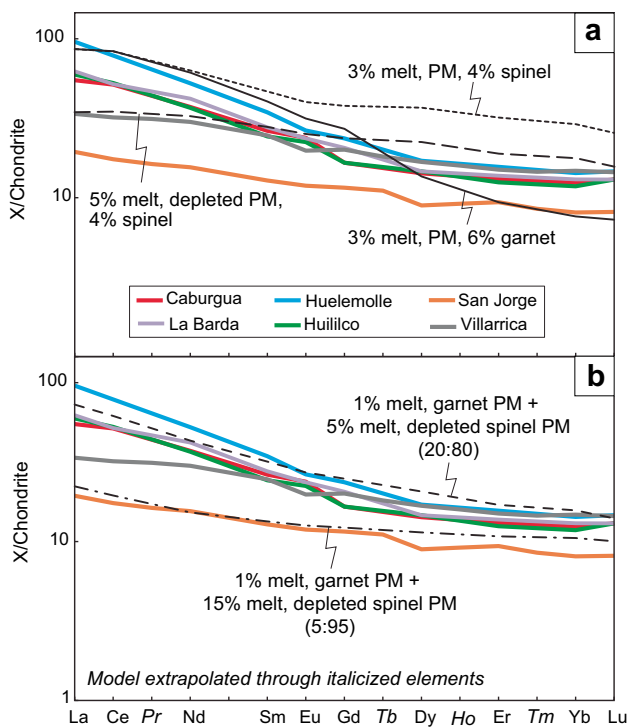


**Fig. 9** REE melting model for the Pucón SECs and Villarrica (samples with the highest MgO (>7 wt% except Huelemolle (5.7 wt%) content plotted). All model parameters are given in the electronic appendix. All starting compositions are based on the primitive mantle composition of Hofmann (1988). Partition coefficients are from the Geochemical Earth Reference Model (GERM) website and Adam and Green (2011), and melting proportions are from Thirlwall et al. (1994). **a** REE patterns cannot be reproduced by sole melting of either garnet-bearing or spinel-bearing mantle, instead, **b** mixing of a small-degree melt of garnet peridotite with a larger-degree melt (3–15%) of spinel peridotite in various proportions can replicate the patterns, with Huelemolle requiring a larger proportion of melt from garnet peridotite, and San Jorge requiring a large degree melt of spinel peridotite. See text for discussion of model

basalt melt inclusions, particularly samples which represent a more primitive melt consisting of higher MgO, lower TiO<sub>2</sub> and undegassed S, which are thought to mix with a more evolved melt before reaching the surface (Saito et al. 2010). Water-rich components identified only in selected volcanic centres as we see in the Pucón area have been identified in numerous other arc basalts, such as in the melt inclusion study of Pagan volcano in the Mariana arc (Tamura et al. 2014) and SECs in the Cascades (Borg et al. 1997; Rowe et al. 2009). These signatures have in some cases been linked to physical location in the arc, as in back arc basin basalts of the Lau Basin, where water-rich components were identified in whole rock analyses closer to the arc only, whereas basalts further away are more similar to Mid Ocean Ridge Basalt (Peate et al. 2001). Such a trend is not seen in the Pucón data (Fig. 7), suggesting that this feature is not universally linked to distance from the trench.

Regionally, the similarity in the melt inclusion Cl/K and K<sub>2</sub>O/TiO<sub>2</sub> (Fig. 6e) and whole rock Sr–Nd isotopic compositions of San Jorge and Lonquimay samples (0.703952 and 0.512880 Jacques et al. 2014 for Lonquimay, see Fig. 5a for San Jorge range) lends further support for the presence of volatile-rich, depleted mantle as the source of San Jorge magmas. This is the first time that this source in Chile has been sampled by a monogenetic volcano. Lonquimay is a stratovolcano north of the Villarrica area (Fig. 1a) thought to be generated from high degree melts of a depleted, fluid-enriched mantle source (Wehrmann et al. 2014). We suggest that this is a mantle source type that is more abundant in Southern Chile than previously recognised, and one which extends further to the east of the arc than predicted from other studies (e.g. Peate et al. 2001). On the scale of the SVZ this depleted, fluid-enriched source is clearly implicated in melting in other locations (see SVZ field in Fig. 8). Variations in melt inclusion Cl content between Villarrica and San Jorge (c. 500–600 ppm) and Lonquimay (900–1000 ppm, Wehrmann et al. 2014) may be due to regional differences in the fluid composition or degree of melting. This fluid is likely to be from dehydrated oceanic crust as its Sr–Nd isotopic composition lies towards that of the altered oceanic crust of Jacques et al. (2014) (Fig. 5a). If the slight positive trend in (<sup>238</sup>U/<sup>232</sup>Th) vs. (<sup>230</sup>Th/<sup>232</sup>Th) is taken as an isochron rather than a mixing line (the latter is unlikely given the lack of linear trends in major and trace element contents, Figs. 2 and 3), the age of fluid addition can be calculated as approximately 8500 years ago (Fig. 5c) suggesting that melting and ascent was almost instantaneous after fluid addition to the source region (c.f. Turner et al. 2001). This shows that fluid-enriched mantle has the power to generate small volume magma batches which ascend sufficiently rapidly that it is relatively unaffected by other processes.

### Determining the effects of shallow-level processes

Source and melting characteristics have been deduced from a combination of U–Th and Sr–Nd isotopes and REE models. However, some features remain unexplained by source processes which must have been gained once the individual magma batches left their melting region.

#### Fractional crystallisation

Major and trace element variations (Figs. 2 and 3) suggest that while fractional crystallisation is clearly occurring locally within the magma systems of individual SECs, broader correlations across the volcanic field require a more complex petrogenesis. The general linear trend in Cr vs. MgO (Fig. 3a) and vertical trend Cr vs. Zr (Fig. 8d) are evidence that olivine crystallisation has occurred, and

this is also evident from comparison of whole rock and melt inclusion compositions as seen by the lower  $\text{SiO}_2$  in the latter (Fig. 6b). Villarrica is the only centre where samples have a small negative Eu anomaly (Fig. 4b), suggesting crystallisation of plagioclase, although major element trends in  $\text{Al}_2\text{O}_3$ ,  $\text{Na}_2\text{O}$  and  $\text{K}_2\text{O}$  are not particularly strong (see vectors on Fig. 2). Despite being represented by the fewest number of samples in the data set, Huelemolle lavas show a trend in the majority of the major elements (negative in  $\text{SiO}_2$ ,  $\text{Al}_2\text{O}_3$ ,  $\text{TiO}_2$ ,  $\text{Fe}_2\text{O}_3$ ,  $\text{Na}_2\text{O}$  and  $\text{K}_2\text{O}$  vs.  $\text{MgO}$  and positive in  $\text{CaO}$  vs.  $\text{MgO}$ , Fig. 2), which can be explained by the addition of a small percentage (<10%) of augite to its most 'primitive' starting composition (Fig. 2). This cannot, however, explain the increase of 1 wt%  $\text{SiO}_2$  within Huelemolle samples at constant  $^{87}\text{Sr}/^{86}\text{Sr}$  (Fig. 5b), as this would require the unrealistic addition of 75% augite. Clinopyroxene can also affect the middle-REEs, and the fact that the REE patterns for Huelemolle, Huililco, Caburgua and La Barda are nearly identical suggests that the small amount of crystallisation suggested from clinopyroxene vectors in Fig. 2 does not affect the composition of these lavas to a large degree. The involvement of amphibole as a crystallising or residual mineral is also refuted as middle-REEs do not show the characteristic depletion in the melt commonly associated with this (Fig. 4b), also shown by the  $\text{Dy}/\text{Dy}^*$  vs.  $\text{Dy}/\text{Yb}$  pattern in Fig. 8b (e.g. Davidson et al. 2013).

The high  $\text{MgO}$  nature of San Jorge rocks compared to the other SECs and Villarrica could be interpreted that rocks erupted at this centre represent a parental melt, a hypothesis which could be supported by the fact that San Jorge and Villarrica samples often lie along the same trajectory in major and trace element content. However, we observe that the olivine Fo# of San Jorge is slightly below what is expected for its whole rock Mg# (Sect. 5.3) suggesting that olivine accumulation may have taken place, thus artificially increasing the  $\text{MgO}$  content. Despite this, we suggest that although SECs with lower  $\text{MgO}$  compositions (5 wt%) may represent minor evolution by fractional crystallisation of olivine, San Jorge is unlikely to be parental to such melts due to its similarity in  $\text{SiO}_2$  content (Fig. 2a), and the fact that their Cr vs.  $\text{MgO}$  contents lie along different trajectories (Fig. 3a).

#### *Resolving the effects of crustal contamination from sediment addition using trace element models and olivine-hosted melt inclusions*

Several lines of evidence indicate that Huililco magmas were significantly contaminated by the local basement rocks. As detailed in Sect. 2, basement rocks in the Pucón area are mainly Cretaceous granitoids, which are occasionally found as small (1–2 cm), fresh, angular xenoliths in the

fall sequences of some of the SECs. One granitic and one granodioritic xenolith found within tephra deposits 7 km east of La Barda and within the San Jorge tephra sequence (respectively) were analysed for major and trace element content (Table 2). The granodiorite xenolith (59 wt%  $\text{SiO}_2$ ) has moderate  $\text{K}_2\text{O}$  content (1.78 wt%), relatively high total alkalis, Rb, Th (5.34, 55 and 3.5 ppm, respectively) and very high Ba (795 ppm). The granite xenolith (71 wt%  $\text{SiO}_2$ ) has higher  $\text{K}_2\text{O}$  (3.77 wt%), high total alkalis (7.47) and far higher concentrations of Rb and Th (116 and 11 ppm, respectively). Either basement rock is, therefore, a potential contaminant to the Huililco magmas. Simple mass balance modelling was undertaken using elements (Cr and Zr, Fig. 8d) and element ratios ( $\text{Sr}/\text{Th}$  and  $\text{Th}/\text{Ce}$ , Fig. 8e) in which the SECs and Villarrica compositions form coherent trends with distinct trajectories. Two model lines are shown for mixing with granite, starting from San Jorge-like and La Barda-like compositions: Huililco compositions lie along a very similar trajectory to the latter mixing line (Figs. 8d, e). San Jorge compositions may lie partially on the mixing line with granite or granodiorite suggesting small amounts of assimilation, however, given the strong trends in major element concentrations for this SEC (Fig. 2), this is more likely to signify olivine fractionation in the case of Cr vs. Zr (Fig. 8d) and the enrichment in fluid mobile elements in the case of the elevated  $\text{Sr}/\text{Th}$  (Fig. 8e). Caburgua and La Barda compositions show little evidence of being substantially altered by assimilation of either of these rock types.

Further compelling evidence for crustal contamination at Huililco is that high  $\text{K}_2\text{O}$  and  $\text{SiO}_2$  values observed in whole rock compositions of this centre are also present in the olivine-hosted melt inclusion data. Huililco whole rock and melt inclusion data generally fall within the field of inclusion data for Chilean SVZ stratovolcanoes rather than monogenetic volcanoes, and furthermore, the trend to lower Cl/K with higher  $\text{K}_2\text{O}/\text{TiO}_2$  suggests that crustal contamination occurred before crystallisation of olivine as in the case of Parícutin c.f. Rowe et al. (2011b). Therefore, although the isotopic signature of granite xenoliths is similar to that of Chilean trench sediment (see Fig. 5a) we favour crustal contamination [c.f. Volcán Llaima, (Reubi et al. 2011) and Volcán Mocho-Choshuenco (McMillan et al. 1989)] rather than influence of sediments from the slab at Huililco as the latter is unlikely to be recorded in olivine phenocrysts. The effect of assimilation on compositions may in fact be significantly larger, as we note that the lava samples show far stronger indicators of crustal contamination compared to the scoria (see labelled samples in Figs. 2h and 3c). Villarrica melt inclusion literature data fall into two groups on these figures: one which is partially degassed (low  $\text{K}_2\text{O}$ , S and Cl/K) and one which trends in the same direction as Huililco/Parícutin, which suggests

that at least some of the melts involved in the petrogenesis of Villarrica may have been crustally contaminated. This is also supported by some Villarrica samples lying along a negative trend in Cr vs. Zr—similar to data from Huililco—indicating assimilation of crustal (granitic) rocks (Fig. 8a).

When the Chilean CSVZ data are looked at in closer detail in Cl/K vs.  $K_2O/TiO_2$ , it can be seen that Huililco has a similar trend to stratovolcano inclusion values for volcanic suites where contamination is documented as having taken place: Llaima inclusions occupy a large area, but with a general negative trend which tapers towards Huililco values. It was proposed by Reubi et al. (2011) that the magmas ascending beneath this centre were assimilating the plutonic roots of the complex, leading to dilution of U-series isotopic signals; equilibrium U-Th ratios in some of the Pucón SECs could thus be achieved by assimilation of the basement granites in the same way. This could suggest that Huililco and Huelemolle initially displayed small Th-excesses like their neighbours La Barda and Cabargua, which appear to have a far smaller crustal influence. The fact that Huelemolle and Huililco lie on a trend between secular equilibrium and Cabargua in  $^{87}Sr/^{86}Sr$  vs. ( $^{238}U/^{230}Th$ ) rather than towards the elevated ( $^{238}U/^{230}Th$ ) values of San Jorge and Villarrica may support this (Fig. 5f). Melt inclusion analyses from Volcán Mocho-Choshuenco follow an excellent mixing line in Cl/K vs.  $K_2O/TiO_2$  from the composition of Lonquimay melt inclusions to those from Huililco (Fig. 6e); this further strengthens the case for significant contamination by basement granitoids as these are present as partially melted xenoliths within its deposits (McMillan et al. 1989). Whole rock values of these lavas (from McMillan et al. 1989) additionally show a positive trend in  $SiO_2$  vs.  $K_2O$  similar to Huililco whole rock and melt inclusion compositions (Fig. 6b).

Simple modelling between a less contaminated Huililco melt inclusion and bulk upper crust (using  $K_2O$ ,  $TiO_2$  and Cl values given in Rudnick and Gao 2004, see Fig. 6 caption) is performed and plotted on Fig. 6d. The mixing line produced explains well the trend seen in Huililco melt inclusions (and those from Mocho-Choshuenco (McMillan et al. 1989) and Llaima (Bouvet de Maisonneuve et al. 2012), see Fig. 1a for locations), however, the model predicts up to 50% assimilation. This percentage seems unrealistically large; however, two factors can be taken into account which are not portrayed by this simple model: (1) it has been shown in numerous examples that granites hosted in ascending magma are subject to disequilibrium melting whereby extreme trace element and isotopic compositions of partial melts can be obtained due to the selective fusion of some minerals over others, such as feldspars, (e.g. Grove et al. 1988; Knesel and Davidson 1999; McGee et al. 2015a; McLeod et al. 2012), which may explain the notable trend of the Huililco melt inclusion data to elevated

$K_2O/TiO_2$  at lower Cl/K (Fig. 6d). This may be dependent on, for example, the size and modal mineralogy of the xenolith, as well as the immersion time in the host magma (e.g. Shaw 2009). Support for this is that granite xenoliths at Mocho-Choshuenco are observed as being partially digested (McMillan et al. 1989); and (2) assimilation is most likely not the only process occurring, as seen in the small amounts of fractional crystallisation of olivine crystallisation occurring within the melt inclusions (see model lines on Fig. 6b). We have already shown that fractional crystallisation occurs concomitantly in Huelemolle and some Villarrica magmas, and we show in the following section that fluids are also involved in the petrogenesis of magma in this region, and in some centres this signal dominates compositional characteristics.

The striking correlation between Sr/Th and Th/Ce (Fig. 8e) in Huelemolle samples is strongly indicative of crustal contamination, as is the similarity in Sr–Nd isotopic ratios to Huililco (Fig. 5a), and the elevated  $^{87}Sr/^{86}Sr$  at similar  $SiO_2$  to Cabargua and La Barda in some Huelemolle samples (Fig. 5b). However, the divergence of Huelemolle compositions to higher ( $^{230}Th/^{232}Th$ ) at  $^{87}Sr/^{86}Sr$  ratios similar to San Jorge, Villarrica and Huililco (e.g. Hawkesworth et al. 1997) (Fig. 5e) is evidence that these magmas contain an old component which has evolved to high ( $^{230}Th/^{232}Th$ ) ratios (e.g. Reubi et al. 2011); this component is not noticeably involved in the genesis of the other SECs or Villarrica. Despite the similarity of Sr–Nd isotopic composition of Chilean trench sediment (Lucassen et al. 2010) and granitic xenoliths from Mocho-Choshuenco (McMillan et al. 1989) (Fig. 5a), ratios of Th/La and Sm/La for Huelemolle—which are expected to be enriched in sediments (c.f. Plank 2005)—are the lowest in the SVZ, which is evidence against incorporation of trench sediment being the explanation for this component and instead suggests that it is something quite different.

### Interaction between large scale tectonics and small scale volcanism

The composition of the individual SECs provides insights into the petrogenesis of the whole magmatic system in this area and highlights important interconnections with local tectonics and longer-lived magmatic systems.

#### *Connection to the Liquiñe Ofqui fault system and the prevalence of decompression melting*

Cabargua, La Barda and Huelemolle show a clear subduction influence in their trace element compositions (Fig. 4a) yet lie on the equiline and partially into the

field of Th-excess (Fig. 5b), where U-excess is expected due to the fluid mobility of U. As shown from the REE modelling (Fig. 9), we do not invoke a large influence of residual garnet which could explain a slight Th-excess. Instead, this suggests the overlapping of the melting signature caused by fluid flux from the slab by a decompression melting signal probably due to the tectonic control of the LOFS in SECs aligned with this feature. This could mean that U-Th isotopic signatures indicative of decompression melting become more dominant than those caused by fluids, perhaps in transient episodes of stress drop. Of all the SECs studied here, La Barda and Caburgua show the greatest compositional similarity. This is likely to be due to their position on the LOFS (Figs. 1, 7) as the secondary permeability provided by this fault system (e.g. Sánchez et al. 2013) allows repeated magma ascent through the main and secondary faults during a single eruptive episode, which could result in geochemical overprinting and a certain degree of homogenisation. Their lack of evidence of crustal processing (crystallisation or assimilation) is further support of this.

In their melt inclusion study of monogenetic and stratovolcanoes of the SVZ Wehrmann et al. (2014) observed that compositions within monogenetic rocks aligned with the LOFS are less degassed and have higher volatile contents (Cl and S), suggesting faster magma ascent of less evolved magmas than those feeding stratovolcanoes. This matches with the Pucón SECs from the present study, as although only Caburgua melt inclusions extend to the range seen in S, it is the only one in our melt inclusion dataset aligned with the LOFS (Fig. 7). Interestingly, S contents within olivine-hosted melt inclusions from the intraplate but rift-related Chaîne de Puys volcanic field in the Massif Central also extend to values beyond sulphide saturation (up to 1800 ppm, Jannot et al. 2005) suggesting that in general magmas may be generated under more oxidized conditions or from more fertile sources (*c.f.* Rowe et al. 2009) than those that are fluid-enriched (such as San Jorge) or contaminated (such as Huililco), and that this may be related to the potentially decompression-driven melting regime.

Eight samples from four of the SECs were analysed for major and trace element content and Sr–Nd–Pb isotopes by Hickey-Vargas et al. (1989) as part of a study of the chain of stratovolcanoes, and expanded on with the addition of uranium- (U-) series and  $^{10}\text{Be}/^9\text{Be}$  isotopes and further Sr–Nd–Pb isotopes for Villarrica volcano and six of the SECs (Hickey-Vargas et al. 2002, 2016). In the latter studies it was suggested that several of these SECs had incorporated ancient subduction-related basalts (pyroxenitised), and that this was distinct from the mantle source of San Jorge SEC and Villarrica. It was suggested by Hickey-Vargas et al. (2002, 2016) that the

movement on the LOFS allowed the incorporation of this pyroxenite from previous subduction. We agree that Huelemolle magmas contain a unique component which may be stored on timescales longer than the U-Th decay. Although this can explain the trace element characteristics which are distinct from the other SECs (e.g. low Th/La Fig. 8f) and elevated ( $^{230}\text{Th}/^{232}\text{Th}$ ) ratios (Fig. 5c, e) observed in these samples, we do not see evidence of this in other LOFS centres from the Pucón area, and do not attribute the equilibrium U-Th values of Huililco to this same component.

#### *Connections to the stratovolcanoes Villarrica and Quetrupillán: Fluid-flux melting vs. crustal contamination*

Although in Sect. 6.2.1 we negate a parental link between San Jorge and the other SECs, we observe similarities in the composition of the former with the stratovolcano Villarrica, in particular in its distinctive FME/HFSE ratios (Fig. 4) and its Sr–Nd isotopic content (Fig. 5). Major element compositions of Villarrica lavas in general lie along olivine crystallisation trajectories from San Jorge compositions (Fig. 2), although lower  $\text{TiO}_2$  and alkali element concentrations in the latter suggest that this source may be more depleted than that of Villarrica, or that the latter may simply be a dilute, less extreme version of San Jorge-type melts due to longer-term evolution in a stable magma reservoir (e.g. Morgado et al. 2015). The notable resemblance of the two compositions, however, suggests that the Villarrica mantle source has experienced a similar fluid-enrichment process as San Jorge. High FME concentrations in Villarrica and Llaima are suggested by Wehrmann et al. (2014) to result from the subduction and subsequent water release from lower oceanic crust which became hydrated due to seawater infiltration at the Valdivia Fracture Zone, a structural feature which coincides with these stratovolcanoes. A fluid-enriched, depleted source has also been identified under other SVZ volcanoes such as Lonquimay, which has olivine-hosted melt inclusion compositions similar to those of San Jorge (Fig. 6e). The San Jorge melting regime may have exploited a particularly fluid-enriched part of this which ascended rapidly, limiting the interaction with basement rocks or encouraging stalling of the magma body.

We note that melt inclusion and whole rock compositions of Villarrica literature data fall into two groups: one has more degassed melt inclusion compositions and the other has melt inclusion compositions that are not degassed, lie towards the same trend as Huililco (Fig. 6) and show some trace element evidence of contamination by basement granite (Fig. 8d, e). It was noted in a previous melt inclusion study of historic Villarrica eruptions by Witter et al.

(2004) that the majority of the magma was degassed and that this was probably due to the presence of a lava lake (still present in 2016). As U-Th isotopes are only available from the most recent eruptions of Villarrica (this study and Sigmarsson et al. 2002), it is not known how much this open system behaviour affects the isotopic disequilibria (*c.f.* Hughes and Hawkesworth 1999). However, the presence of a population of undegassed inclusions and some evidence of crustal contamination shows the likelihood that some closed system processes occur, and that these may be similar to those affecting the smaller melting events which give rise to the SECs.

The crustal contamination modelled for the Huililco magmas hints towards a different type of SEC-stratovolcano connection to that of San Jorge and Villarrica. The fact that sufficient heat was available for assimilation to occur and be recorded as contaminated melts within olivine crystals (*i.e.* before any fractional crystallisation took place) suggests that Huililco—despite being an isolated SEC—may be connected to one of the larger magmatic systems, such as that of nearby Quetrupillán stratovolcano (Fig. 1) with which it shares the same Sr–Nd isotopic composition (Fig. 5a). The lower Fo# olivines which are out of equilibrium with the Huililco whole rock composition are further evidence of this (“Olivine and olivine-hosted melt inclusion analyses”), and this hypothesis also explains the presence of plagioclase crystals with disequilibrium textures (Sect. 4), a feature which is not observed in rocks from the other SECs.

### The scale of heterogeneity: arc-scale implications from small-volume basalts

Detailed study of the Pucón magmatic system using a combination of published isotopic data and new whole rock major and trace element, U-Th isotopic and olivine-hosted melt inclusion has shown important compositional variations linked to competing regional magmatic and tectonic controls. Despite being produced from a similar source we show that individual SEC compositions are the result of varying deep and shallow processes. Those aligned with a large scale strike-slip fault show evidence of ascending by decompression melting (La Barda and Caburgua), whilst other, isolated, centres are variably affected by crustal contamination prior to olivine crystallisation (Huililco) and fluid input from the subducting slab which aided more extensive melting and rapid ascent (San Jorge).

The distinct compositional signatures of San Jorge and Huililco despite their proximity to each other and almost equal distance from the arc front shows that a general model of compositional changes across the arc cannot be applied to the Pucón system, or that such models cannot

be applied to large datasets over small areas. We also show that connections between SECs and stratovolcanoes are not predictable: San Jorge and Villarrica may share the same source component and behaviour, whilst Quetrupillán and Huililco may share a plumbing system or magmatic history.

We have shown that compositions of mafic material erupted in SECs represent snapshots in time of mantle and crustal processes, which may be overprinted in larger volcanic systems or simply missed by under-sampling. Their heterogeneity also provides evidence for the isolation of small volume, short duration melting events and their ascent paths (McGee et al. 2015b; Rasoazanamparany et al. 2015; Watt et al. 2013), even if they do not rise rapidly from the mantle (as must be the case for the contaminated compositions of Huililco). The differences in major and trace element compositions highlighted in several centres within individual eruption sequences also shows that heterogeneity is observed on the scale of a single melting event and possibly during ascent of the resultant magma batch. Further in-depth studies of individual sequences will be required to quantitatively ascertain on what timescale these may occur.

Compositional heterogeneity occurs at a variety of depths: from the initiating of melting by fluid and sediment input to the mantle wedge, decompression melting caused by large tectonic structures, to crustal contamination prior to crystal fractionation. A notable observation is that in most geochemical parameters the heterogeneity seen in the Pucón region is present in the whole of the SVZ of Chile, in monogenetic or polygenetic volcanoes. This is seen in the SVZ-wide data plotted in Fig. 5 (Sr–Nd isotopes), Fig. 6 (melt inclusions) and Fig. 8 (trace elements), where the data mirror the ‘end-members’ investigated in the present study. Therefore, small eruptive centres are an effective probe of deep (source related) and shallow processes which are occurring on a larger, regional scale, and our approach combining several geochemical techniques has been effective in identifying these details.

We suggest that the smaller the magma batch, the greater the possibility of preserving details of the melting event. The fact that such a variety in geochemistry is observed for the Pucón area lies in the design of our study in selecting small eruptive centres rather than focussing on stratovolcanoes. Clearly there is a threshold size whereby above this limit certain geochemical signals are overprinted or homogenised (*c.f.* McGee et al. 2015b). Villarrica is an excellent example of this: detailed study of this small area has identified that this longer-lived, active stratovolcano has genetic similarities to the SEC San Jorge, although its distinctive depleted, fluid-enriched signal (seen in ( $^{238}\text{U}/^{232}\text{Th}$ ) Fig. 5c, f, and  $\text{Dy}/\text{Dy}^*$  vs.  $\text{Dy}/\text{Yb}$ , Fig. 8a) has been modified by fractional crystallisation (Fig. 2) and limited crustal contamination (seen in melt inclusions analyses of  $\text{K}_2\text{O}$  vs.  $\text{SiO}_2$  and  $\text{Cl}/\text{K}$  vs.  $\text{K}_2\text{O}/$

TiO<sub>2</sub>, Fig. 6b and d, and trace element modelling, Fig. 8d, e). In this way, understanding the genesis of small volume volcanoes in arcs provides us with vital information on how larger, long-lived volcanic systems form and evolve.

**Acknowledgments** This Project was financed by FONDECYT Grant 11130296 to LM, who was supported at CEGA by FONDAP Project 15090013. HH acknowledges support from an Australian Research Council Future Fellowship, FT120100440. NV acknowledges financial support from CONICYT/FONDECYT grant #3140353. LL acknowledges former support from FONDECYT grant 1107022. We thank Ian Smith and John Adam for helpful comments regarding high Mg andesites, and Gerhardt Woerner for many helpful discussions regarding Chilean volcanoes. Roberto Topp, Tomás Martínez and Andrés Flores are thanked for their help and enthusiasm in the field, and Roberto Valles and Anisse Pizarro for their excellent work in sample preparation. We thank the editor Tim Grove and two anonymous reviewers for their detailed and constructive comments, and Leonid Danyushevsky, John Gamble and an anonymous reviewer for their useful comments on a previous version of this paper.

## References

- Adam J, Green T (2011) Trace element partitioning between mica- and amphibole-bearing garnet lherzolite and hydrous basanitic melt: 2. Tasmanian Cainozoic basalts and the origins of intra-plate basaltic magmas. *Contrib Miner Petrol* 161(6):883–899
- Ariskin AA, Bychkov KA, Danyushevsky LV, McNeill AW, Barmina GS, Nikolaev GS (2012) COMAGMAT-5: a new magma crystallization model designed to simulate mafic to ultramafic sulfide-saturated systems. In: Abs. 12th international Ni–Cu–(PGE) symposium (June 16–21, 2012, Guiyang, China), p 15–18
- Arndt N (2003) Komatiites, kimberlites, and boninites. *J Geophys Res Solid Earth* 108(B6). doi:10.1029/2002JB002157
- Blondes MS, Reiners PW, Ducea MN, Singer BS, Chesley J (2008) Temporal-compositional trends over short and long time-scales in basalts of the Big Pine Volcanic Field, California. *Earth Planet Sci Lett* 269:140–154
- Borg LE, Clyne MA, Bullen TD (1997) The variable role of slab-derived fluids in the generation of a suite of primitive calc-alkaline lavas from the southernmost Cascades, California. *Can Miner* 35:425–452
- Bouvet de Maisonneuve C, Dungan MA, Bachmann O, Burgisser A (2012) Insights into shallow magma storage and crystallization at Volcán Llaima (Andean Southern Volcanic Zone, Chile). *J Volcanol Geoth Res* 211–212:76–91
- Brenna M, Cronin S, Smith I, Sohn Y, Németh K (2010) Mechanisms driving polymagmatic activity at a monogenetic volcano, Udo, Jeju Island, South Korea. *Contrib Miner Petrol* 160(6):931–950
- Brenna M, Cronin SJ, Smith IEM, Maas R, Sohn YK (2012) How Small-volume Basaltic Magmatic Systems Develop: a Case Study from the Jeju Island Volcanic Field, Korea. *J Petrol* 53(5):985–1018
- Bucchi F, Lara LE, Gutiérrez F (2015) The Carrán-Los Venados Volcanic Field and its relationship with coeval and nearby polygenetic volcanism in an intra-arc setting. *J Volcanol Geoth Res* 308:70–81
- Cameron W, McCulloch M, Walker D (1983) Boninite petrogenesis: chemical and Nd-Sr isotopic constraints. *Earth Planet Sci Lett* 65(1):75–89
- Cembrano J, Lara L (2009) The link between volcanism and tectonics in the southern volcanic zone of the Chilean Andes: a review. *Tectonophysics* 471(1–2):96–113
- Cembrano J, Hervé F, Lavenu A (1996) The Liquiñe Ofqui fault zone: a long-lived intra-arc fault system in southern Chile. *Tectonophysics* 259(1–3):55–66
- Cheng H, Lawrence Edwards R, Shen C-C, Polyak VJ, Asmerom Y, Woodhead J, Hellstrom J, Wang Y, Kong X, Spötl C, Wang X, Calvin Alexander E Jr (2013) Improvements in <sup>230</sup>Th dating, <sup>230</sup>Th and <sup>234</sup>U half-life values, and U-Th isotopic measurements by multi-collector inductively coupled plasma mass spectrometry. *Earth Planet Sci Lett* 371–372:82–91
- Conrey RM, Sherrod DR, Hooper PR, Swanson DA (1997) Diverse primitive magmas in the Cascade arc, northern Oregon and southern Washington. *Can Miner* 35:367–396
- Cooper LB, Plank T, Arculus RJ, Hauri EH, Hall PS, Parman SW (2010) High-Ca boninites from the active Tonga Arc. *J Geophys Res Solid Earth* 115(B10). doi:10.1029/2009JB006367
- Costantini L, Pioli L, Bonadonna C, Clavero J, Longchamp C (2011) A late Holocene explosive mafic eruption of Villarrica volcano, Southern Andes: the Chaimilla deposit. *J Volcanol Geoth Res* 200(3–4):143–158
- Danyushevsky LV, Della-Pasqua FN, Sokolov S (2000) Re-equilibration of melt inclusions trapped by magnesian olivine phenocrysts from subduction-related magmas: petrological implications. *Contrib Miner Petrol* 138:68–83
- Davidson J, Turner S, Plank T (2013) Dy/Dy\*: variations arising from Mantle sources and petrogenetic processes. *J Petrol* 54(3):525–537
- Gamble J, Wood C, Price R, Smith I, Stewart R, Waight T (1999) A fifty year perspective of magmatic evolution on Ruapehu Volcano, New Zealand: verification of open system behaviour in an arc volcano. *Earth Planet Sci Lett* 170(3):301–314
- Grove TL, Kinzler RJ, Baker MB, Donnelly-Nolan JM, Leshner CE (1988) Assimilation of granite by basaltic magma at Burnt Lava flow, Medicine Lake volcano, northern California: decoupling of heat and mass transfer. *Contrib Miner Petrol* 99(3):320–343
- Haase KM, Renno AD (2008) Variation of magma generation and mantle sources during continental rifting observed in Cenozoic lavas from the Eger Rift, Central Europe. *Chem Geol* 257(3–4):192–202
- Hawkesworth CJ, Turner SP, McDermott F, Peate DW, van Calsteren P (1997) U-Th isotopes in Arc Magmas: implications for element transfer from the subducted crust. *Science* 276(5312):551–555
- Hickey-Vargas R, Roa HM, Escobar LL, Frey FA (1989) Geochemical variations in Andean basaltic and silicic lavas from the Villarrica-Lanin volcanic chain (39.5°S): an evaluation of source heterogeneity, fractional crystallization and crustal assimilation. *Contrib Miner Petrol* 103(3):361–386
- Hickey-Vargas R, Sun M, López-Escobar L, Moreno-Roa H, Reagan MK, Morris JD, Ryan JG (2002) Multiple subduction components in the mantle wedge: evidence from eruptive centers in the Central Southern volcanic zone, Chile. *Geology* 30(3):199–202
- Hickey-Vargas R, Sun M, Holbik S (2016) Geochemistry of basalts from small eruptive centers near Villarrica stratovolcano, Chile: evidence for lithospheric mantle components in continental arc magmas. *Geochim Cosmochim Acta* 185:358–382
- Hofmann AW (1988) Chemical differentiation of the Earth: the relationship between mantle, continental crust, and oceanic crust. *Earth Planet Sci Lett* 90(3):297–314
- Huang F, Xu J, Zhang J (2016) U-series disequilibria in subduction zone lavas: inherited from subducted slabs or produced by mantle in-growth melting? *Chem Geol* 440:179–190
- Hughes RD, Hawkesworth CJ (1999) The effects of magma replenishment processes on <sup>238</sup>U-<sup>230</sup>Th disequilibrium. *Geochim Cosmochim Acta* 63(23–24):4101–4110
- Jacques G, Hoernle K, Gill J, Wehrmann H, Bindeman I, Lara LE (2014) Geochemical variations in the Central Southern Volcanic



- Zone, Chile (38–43 S): the role of fluids in generating arc magmas. *Chem Geol* 371:27–45
- Jannot S, Schiano P, Boivin P (2005) Melt inclusions in scoria and associated mantle xenoliths of Puy Beauvit Volcano, Chaîne des Puys, Massif Central, France. *Contrib Miner Petrol* 149(5):600–612
- Jicha BR, Singer BS, Beard BL, Johnson CM, Moreno-Roa H, Naranjo JA (2007) Rapid magma ascent and generation of <sup>230</sup>Th excesses in the lower crust at Puyehue-Cordón Caulle, Southern Volcanic Zone, Chile. *Earth Planet Sci Lett* 255(1–2):229–242
- Jordan SC, Jowitt SM, Cas RAF (2015) Origin of temporal—compositional variations during the eruption of Lake Purrumbete Maar, Newer Volcanics Province, southeastern Australia. *Bull Volcanol* 77(1):1–15
- Knesel KM, Davidson JP (1999) Sr isotope systematics during melt generation by intrusion of basalt into continental crust. *Contrib Miner Petrol* 136(3):285–295
- Lara LE, Lavenu A, Cembrano J, Rodríguez C (2006) Structural controls of volcanism in transversal chains: resheared faults and neotectonics in the Cordón Caulle-Puyehue area (40.5°S), Southern Andes. *J Volcanol Geoth Res* 158(1–2):70–86
- Leeman WP, Lewis JF, Everts RC, Conrey RM, Streck MJ (2005) Petrologic constraints on the thermal structure of the Cascades arc. *J Volcanol Geoth Res* 140(1–3):67–105
- López-Escobar L, Cembrano J, Moreno H (1995) Geochemistry and tectonics of the Chilean Southern Andes basaltic Quaternary volcanism (37–46°S). *Andean Geol* 22(2):219–234
- Lucassen F, Wiedicke M, Franz G (2010) Complete recycling of a magmatic arc: evidence from chemical and isotopic composition of quaternary trench sediments in Chile (36–40 S). *Int J Earth Sci (Geol Rundsch)* 99(3):687–701
- Lundstrom CC (2003) Uranium-series disequilibria in mid-ocean ridge basalts: observations and models of basalt genesis. *Rev Miner Geochem* 52(1):175–214
- McDonough WF, Sun S-s (1995) The composition of the Earth. *Chem Geol* 120:223–253
- McGee LE, Smith IEM (2016) Interpreting chemical compositions of small scale basaltic systems: a review. *J Volcanol Geoth Res* 325:45–60
- McGee LE, Millet M-A, Smith IEM, Németh K, Lindsay JM (2012) The inception and progression of melting in a monogenetic eruption: Motukorea Volcano, the Auckland Volcanic Field, New Zealand. *Lithos* 155:360–374
- McGee LE, McLeod C, Davidson JP (2015a) A spectrum of disequilibrium melting preserved in lava-hosted, partially melted crustal xenoliths from the Wudalianchi volcanic field, NE China. *Chem Geol* 417:184–199
- McGee LE, Millet M-A, Beier C, Smith IEM, Lindsay JM (2015b) Mantle heterogeneity controls on small-volume basaltic volcanism. *Geology* 43(6):551–554
- McLeod CL, Davidson JP, Nowell GM, de Silva SL (2012) Disequilibrium melting during crustal anatexis and implications for modeling open magmatic systems. *Geology* 40(5):435–438
- McMillan NJ, Harmon RS, Moorbath S, Lopez-Escobar L, Strong DF (1989) Crustal sources involved in continental arc magmatism: a case study of volcan Mocho-Choshuenco, southern Chile. *Geology* 17(12):1152–1156
- Moreno H, Clavero J (2006) Geología del volcán Villarrica, Regiones de la Araucanía y de los Lagos. Servicio Nacional de Geología y Minería. Carta Geológica de Chile, Serie Geología Básica. No. 98. Mapa escala 1:50000
- Morgado E, Parada MA, Contreras C, Castruccio A, Gutiérrez F, McGee LE (2015) Contrasting records from mantle to surface of Holocene lavas of two nearby arc volcanic complexes: Caburgua-Huelemolle Small Eruptive Centers and Villarrica Volcano, Southern Chile. *J Volcanol Geoth Res* 306:1–16
- Nielsen RL, Michael PJ, Sours-Page R (1998) Chemical and physical indicators of compromised melt inclusions. *Geochim Cosmochim Acta* 62(5):831–839
- Peate DW, Kokfelt TF, Hawkesworth CJ, Van Calsteren PW, Hergt JM, Pearce JA (2001) U-series Isotope data on Lau Basin glasses: the role of subduction-related fluids during melt generation in Back-arc Basins. *J Petrol* 42(8):1449–1470
- Pioli L, Scalisi L, Costantini L, Di Muro A, Bonadonna C, Clavero J (2015) Explosive style, magma degassing and evolution in the Chaimilla eruption, Villarrica volcano, Southern Andes. *Bull Volcanol* 77(11):1–14
- Plank T (2005) Constraints from thorium/lanthanum on sediment recycling at subduction zones and the evolution of the continents. *J Petrol* 46(5):921–944. doi:10.1093/petrology/egi005
- Price RC, Turner S, Cook C, Hobden B, Smith IEM, Gamble JA, Handley H, Maas R, Möbis A (2010) Crustal and mantle influences and U-Th-Ra disequilibrium in andesitic lavas of Ngauruhoe volcano, New Zealand. *Chem Geol* 277(3–4):355–373
- Rasoazanamparany C, Widom E, Valentine G, Smith E, Cortés J, Kuentz D, Johnsen R (2015) Origin of chemical and isotopic heterogeneity in a mafic, monogenetic volcanic field: a case study of the Lunar Crater Volcanic Field, Nevada. *Chem Geol* 397:76–93
- Reagan MK, Gill JB (1989) Coexisting calcalkaline and high-niobium basalts from Turrialba Volcano, Costa Rica: implications for residual titanates in arc magma sources. *J Geophys Res Solid Earth* 94(B4):4619–4633
- Reubi O, Bourdon B, Dungan MA, Koornneef JM, Sellés D, Langmuir CH, Aciego S (2011) Assimilation of the plutonic roots of the Andean arc controls variations in U-series disequilibria at Volcan Llaima, Chile. *Earth Planet Sci Lett* 303(1–2):37–47
- Roeder PL, Emslie RF (1970) Olivine-liquid equilibrium. *Contrib Miner Petrol* 29:275–289
- Rowe MC, Nielsen RL, Kent AJ (2006) Anomalously high Fe contents in rehomogenized olivine-hosted melt inclusions from oxidized magmas. *Am Miner* 91(1):82–91
- Rowe MC, Kent AJR, Nielsen RL (2009) Subduction influence on oxygen fugacity and trace and volatile elements in basalts across the Cascade Volcanic Arc. *J Petrol* 50(1):61–91
- Rowe MC, Peate DW, Newbrough A (2011a) Compositional and thermal evolution of olivine-hosted melt inclusions in small-volume basaltic eruptions: a “simple” example from Dotsero Volcano, NW Colorado. *Contrib Miner Petrol* 161:197–211
- Rowe MC, Peate DW, Ukstins Peate I (2011b) An investigation into the nature of the magmatic plumbing system at Parícutin Volcano, Mexico. *J Petrol* 52(11):2187–2220
- Rudnick RL, Gao J (2004) Composition of the continental crust. In: Holland HD, Turekian KK (eds) *Treatise on Geochemistry*, vol 3. Elsevier, Amsterdam, pp 1–64
- Ruprecht P, Bergantz GW, Cooper KM, Hildreth W (2012) The crustal magma storage system of Volcán Quizapu, Chile, and the effects of magma mixing on magma diversity. *J Petrol* 53(4):801–840
- Saito G, Morishita Y, Shinohara H (2010) Magma plumbing system of the 2000 eruption of Miyakejima volcano, Japan, deduced from volatile and major component contents of olivine-hosted melt inclusions. *J Geophys Res Solid Earth* 115(B11). doi:10.1029/2010JB007433
- Salter VJ, Stracke A (2004) Composition of the depleted mantle. *Geochem Geophys Geosyst* 5(5):Q05004. doi:10.1029/2003GC000597
- Sánchez P, Pérez-Flores P, Arancibia G, Cembrano J, Reich M (2013) Crustal deformation effects on the chemical evolution of geothermal systems: the intra-arc Liquiñe-Ofqui fault system, Southern Andes. *Int Geol Rev* 55(11):1384–1400

- Shaw CSJ (2009) Caught in the act—the first few hours of xenolith assimilation preserved in lavas of the Rockeskyllerkopf volcano, West Eifel, Germany. *Lithos* 112(3–4):511–523
- Siebe C, Rodriguez-Lara V, Schaaf P, Abrams M (2004) Geochemistry, Sr-Nd isotope composition, and tectonic setting of Holocene Pelado, Guespalapa and Chichinautzin scoria cones, south of Mexico City. *J Volcanol Geoth Res* 130:197–226
- Sigmarrsson O, Chmeleff J, Morris J, Lopez-Escobar L (2002) Origin of  $^{226}\text{Ra}$ – $^{230}\text{Th}$  disequilibria in arc lavas from southern Chile and implications for magma transfer time. *Earth Planet Sci Lett* 196(3–4):189–196
- Sobolev AV, Chaussidon M (1996)  $\text{H}_2\text{O}$  concentrations in primary melts from supra-subduction zones and mid-ocean ridges: implications for  $\text{H}_2\text{O}$  storage and recycling in the mantle. *Earth Planet Sci Lett* 137(1):45–55
- Sun S-s, McDonough WF (1989) Chemical and isotopic systematics of oceanic basalts: implications for mantle composition and processes. *Geol Soc Lond Spec Publ* 42(1):313–345
- Stern RJ, Morris J, Bloomer SH, Hawkins JW Jr (1991) The source of the subduction component in convergent margin magmas: trace element and radiogenic isotope evidence from Eocene boninites, Mariana forearc. *Geochim Cosmochim Acta* 55(5):1467–1481
- Stracke A, Bizimis M, Salters VJM (2003) Recycling oceanic crust: quantitative constraints. *Geochem Geophys Geosyst* 4(3):8003. doi:10.1029/2001GC00023
- Strong M, Wolff J (2003) Compositional variations within scoria cones. *Geology* 31(2):143–146
- Sun M (2001) Geochemical variation among small eruptive centers in the central SVZ of the Andes: an evaluation of subduction, mantle and crustal influences. Florida International University, Miami
- Tamura Y, Ishizuka O, Stern RJ, Nichols ARL, Kawabata H, Hirahara Y, Chang Q, Miyazaki T, Kimura J-I, Embley RW, Tatsumi Y (2014) Mission Immiscible: distinct subduction components generate two primary Magmas at Pagan Volcano, Mariana Arc. *J Petrol* 55(1):63–101
- Tašárová ZA (2007) Towards understanding the lithospheric structure of the southern Chilean subduction zone (36°S–42°S) and its role in the gravity field. *Geophys J Int* 170(3):995–1014
- Thirlwall MF, Upton BGJ, Jenkins C (1994) Interaction between continental lithosphere and the Iceland Plume—Sr-Nd-Pb Isotope Geochemistry of Tertiary Basalts, NE Greenland. *J Petrol* 35(3):839–879
- Turner S, Evans P, Hawkesworth C (2001) Ultrafast source-to-surface movement of melt at island arcs from  $^{226}\text{Ra}$ – $^{230}\text{Th}$  systematics. *Science* 292:1363–1366
- Turner S, Beier C, Niu Y, Cook C (2011) U-Th-Ra disequilibria and the extent of off-axis volcanism across the East Pacific Rise at 9°30N, 10°30N, and 11°20N. *Geochem Geophys Geosyst* 12(7):Q0AC12
- Valdivia Muñoz PA (2016) Estudio petrológico y geoquímico del Volcán Huililco, IX Región, Chile. Unpublished undergraduate thesis, Universidad de Chile
- Wallace PJ, Carmichael ISE (1999) Quaternary volcanism near the Valley of Mexico: implications for subduction zone magmatism and the effects of crustal thickness variations on primitive magma compositions. *Contrib Miner Petrol* 135(4):291–314
- Watt SFL, Pyle DM, Mather TA, Naranjo JA (2013) Arc magma compositions controlled by linked thermal and chemical gradients above the subducting slab. *Geophys Res Lett* 40(11):2550–2556
- Wehrmann H, Hoernle K, Jacques G, Garbe-Schönberg D, Schumann K, Mahlke J, Lara LE (2014) Volatile (sulphur and chlorine), major, and trace element geochemistry of mafic to intermediate tephra from the Chilean Southern Volcanic Zone (33–43 S). *Int J Earth Sci (Geol Rundsch)* 103(7):1945–1962
- Witter JB, Kress VC, Delmelle P, Stix J (2004) Volatile degassing, petrology, and magma dynamics of the Villarrica Lava Lake, Southern Chile. *J Volcanol Geoth Res* 134(4):303–337